Construction and Building Materials 294 (2021) 123607

Contents lists available at ScienceDirect

Construction and Building Materials

journal homepage: www.elsevier.com/locate/conbuildmat

Characteristics of hemp fibre reinforced foam concretes with fly ash and Taguchi optimization

Osman Gencel [a,*], Oguzhan Yavuz Bayraktar [b], Gokhan Kaplan [c], Ahmet Benli [d], Gonzalo Martínez-Barrera [e], Witold Brostow [f,*], Murat Tek [g], Burak Bodur [b]

[a] Civil Engineering Department, Bartin University, 74100 Bartin, Turkey
[b] Civil Engineering Department, Kastamonu University, 37150 Kastamonu, Turkey
[c] Civil Engineering Department, Ataturk University, 25030 Erzurum, Turkey
[d] Civil Engineering Department, Bingol University, 12100 Bingol, Turkey
[e] Laboratorio de Investigación y Desarrollo de Materiales Avanzados (LIDMA), Facultad de Química, Universidad Autónoma del Estado de México, km. 12 de la carretera Toluca-Atlacomulco, San Cayetano 50200, Mexico
[f] Laboratory of Advanced Polymers and Optimized Materials (LAPOM), Department of Materials Science and Engineering, University of North Texas, 3940 North Elm Street, Denton, TX 76207, USA
[g] Material Science and Engineering Department, Kastamonu University. 37150 Kastamonu, Turkey

HIGHLIGHTS

- With increasing Foam content, the mixtures revealed higher slump values due to decreasing solid content.
- Porosity and water absorption of 28 aged-foam concretes increased with increasing foam content.
- As the foam content increases, the compressive strength of the mixtures decreases.
- Hemp fiber reduced drying shrinkage of foam concretes.
- It has been observed that glass fiber improves the durability properties of foam concretes.

ARTICLE INFO

Article history:
Received 14 February 2021
Received in revised form 13 April 2021
Accepted 9 May 2021

Keywords:
Foam concrete
Fly ash
Hemp fibers
Physico-mechanical properties
Durability properties
Taguchi optimization

ABSTRACT

This study presents investigation on microstructural, mechanical, durability and thermal characteristics of hemp fibers (HFs) reinforced foam concrete with fly ash (FA) and Taguchi optimization approach. Three series of foam concretes mixtures were produced with foam contents of 50, 75 and 100 kg/m^3. There is a reference mixture without HFs and FA. Thus, mixtures contain FA as cement replacement at the concentrations of 0%, 10%, 20%, 30%, 40% and 50%. HFs with varying fiber length were introduced into mixes at concentrations of 0.75%, 1.5% and 3% by weight of cement. Slump test was done to see workability. Compression and flexural properties were determined at 7, 28 and 91 days. Durability was investigated by high temperature, freeze–thaw and sulphate exposures. Thermal conductivity, drying shrinkage, porosity, water absorption and dry unit weight properties of foam concretes were also investigated. Experimental results were analyzed using Taguchi optimization approach. Addition of HFs provides very large compressive and flexural strength enhancements. FA addition reduces the drying shrinkage and thermal conductivity while it increases the high temperature resistance of foam concretes.

1. Introduction

Foam concrete is highly porous composite up to 80% and even more by volume of mixture. Cement, water, filler and voids are trapped in composites via suitable synthetic- or protein-based foaming agents that does not contain coarse aggregate [1–5]. It has advantages such as minimum aggregate consumption, high fluidity and porosity, good thermal isolation, low self-weight, fire resistance, airborne sound insulation, and desired strength and cost effectiveness. Foam concrete is commonly used in panels, walls, road fill, partitions blocks, insulated wall panels, bridge padding, floor insulation, roof insulation and lightweight building blocks in many countries. Foam concrete also became a favorable composite for applications such as weak soils stabilization, a base

* Corresponding authors.
E-mail addresses: ogencel@bartin.edu.tr, osmangencel@gmail.com (O. Gencel), brostow@unt.edu (W. Brostow).

https://doi.org/10.1016/j.conbuildmat.2021.123607
0950-0618/

layer for foundation slabs, floors, subway and highway engineering applications [1,3,6–11]. There is a continuous investigations to obtain alternative concrete-making materials involving economic, environmental and social aspects to achieve sustainable development [12,13]. For this reason, reuse of wastes like fly ash, silica fume, rice husk ash etc. [14,15], silica fume [16], waste marble dust [16–18] and ground blast furnace slag [19,20] as cement substitutes and aggregates is used in concrete. Inclusion of the wastes improves concrete performance provides environmental advantage and reduces CO_2 emissions [21,22].

Like all other concretes, foam concretes have lower tensile strength than the compressive strength, in addition they are subject to massive shrinkage caused by large amounts of entrained air. The use of different fibers and wastes like waste marble dust, silica fume and fly ash in concrete mixtures decreases shrinkage crack and increases durability and strength. Steel, synthetic and glass fibers are widely considered in concrete. Transition of concrete from brittle to semi-ductile or to ductile characteristic, enhanced energy absorption capacity and toughness can be obtained by fiber reinforcement. Such reinforcement (steel, glass or synthetic fibers) can significantly decrease cracking and permeability due to drying shrinkage and plastic shrinkage; the impact and wear resistances are enhanced and strain ability is much improved [6,23]. However, since fiber production causes high pollution and CO_2 emissions, we need to develop new methods for producing energy-efficient fiber-reinforced concretes to increase environmental sustainability. Much research has tested usage of natural, mineral-derived, animal-based and plant-based fibers to reinforce concrete – what involves relatively little energy for extraction from the source [24].

Among natural fibers, hemp fibers (HFs) are the most common and used in biofuels, textile, food, construction, automobile etc. Those fibers found application in the construction industry as lime-hemp plaster, isolation, hemp concrete and polymeric hemp-based composites [25–27]. Çomak et al. [28] investigated mortars produced with different rates and lengths of HFs to evaluate strengths, unit weight, absorption and splitting tensile strength. They pointed out that the optimum results were obtained for 2–3% HFs with 12 mm length. Hamzaoui et al. [29] observed that 3% HFs in the mortar minimizes the negative impact on mechanical strength. Ruano et al. [30] focused flexural behavior of cement-based composites having HFs and sugarcane bagasse fibers and found toughness increase by hemp fibers. Hamzaoui et al. [31] studied hemp fibers and carbon nanotubes blended mortars in respect to microstructure and mechanical behavior and noted 10% and 24% compressive and flexural strength improvement, respectively, because of combined usage of wet hemp fibers and carbon nanotubes. There are a few studies on foam concrete incorporating fly ash (FA) [32,33]. Gökçe et al. [34] studied the foam concrete incorporating FA and silica fume and they reported that the addition of FA decreased compressive strength and thermal conductivity of mixes having high-level foam amount but increased in mixtures with lower foam content. Gopalakrishnan et al. [35] examined fly ash and quarry dust blended foam concrete and they found the optimum fly ash content as 20% – 25% for achieving high short-term compressive strength. We have not found in the literature information on synergetic impact of FA and hemp fibers on physico-mechanical, durability and thermal characteristics of foam concrete. Although FA released from power plants affects environmental, its storage cost is pretty expensive. Turkey annually releases about 18 million tons of FA The analogous number for India is about 80 million tons per year. Approximately 600 million tons of fly ash annually are created worldwide [15,36–38]. Only limited amount of fly ash is recycled in cement production and cement based composites. In order to increase recycling, foam concrete is a new option to consider. In the production of foam concrete, generally micro size materials are desired [39,40]. Thus costs are lower since there is no need to the grinding. Moreover, foams have pozzolanic effect that contributes to strength development. For these reasons we have used fly ash in this study. Due to relatively poor tensile properties of cement based composites, large amounts of work have been expended into usage of fibers such as made of steel, polymeric etc. Steel fibers are expensive and corrosive. In the production of poly(vinyl alcohol) and polypropylene fibers, antioxidants and amines have been used – resulting in non-eco-friendly materials. On the other hand, natural fibers such as made from hemp are eco-friendly, renewable, non-corrosive, inexpensive and abundantly and widely available. This makes hemp fibers a suitable alternative to non-renewable, corrosive and expensive synthetic fibers. Studies using hemp fibers in cement-based composites exhibit a potential to improve the energy absorption capacity [41–43], lowering shrinkage [44,45] and improve the impact resistance [46,47]. For these reasons we have used fly ash and hemp fibers. We have not found studies in the literature using hemp fibers in foam concrete production. Thus, we have now used FA and HFs in fabrication of foam concretes. We are particularly concerned with the shrinkage, thermal conductivity, the strength of concrete at longer times and also with its resistance to high temperature exposure, freeze–thaw cycles and sulphate attack. Foam concrete mixes were produced with 50, 75 and 100 kg/m^3 foam content. Each foam concrete mixtures includes reference mixture without HFs and FA while other mixtures contain FA as cement substitute at the rates of 0%, 10%, 20%, 30%, 40% and 50%. HFs with varying fiber length were also added to the mixtures as 0.75%, 1.5% and 3% by weight of cement. Slump test was applied to assess fresh properties. Strength property was determined after 7, 28 and 91 days, while durability was investigated by high temperature exposures, freeze–thaw cycles and sulphate attacks. Thermal conductivity, drying shrinkage, porosity, water absorption and unit weight properties of concretes were studied.

2. Test program

2.1. Materials and methods

2.1.1. Cement

CEM I 42.5R Portland cement (PC) and FA were utilized as binders. Physical and chemical characteristics of cement are seen in Table 1. Water/binder (PC + FA) ratio (w/b) of 0.50 was taken as constant in mixes.

2.1.2. Fly ash (FA)

F class FA having 2750 cm^2/g fineness was utilized as substitute of PC in 10, 20, 30, 40 and 50% by weight. Table 2 illustrates physical and mechanical characteristics of FA.

2.1.3. Hemp fibers (HFs)

HFs have usually the length of 40–45 mm. They contain ~ 9% lignin and pectin, 78% cellulose. Because lignin rate is higher than flax, it has rougher structure [28]. Long hemp fibers were divided to 0.5, 1 and 2 cm. Ratios (0.75%, 1.5% and 3%) and different lengths (0.5, 1 and 2 cm) of HFs were added to foam concrete mixtures. Fig. 1a illustrates SEM images of HFs. Fig. 1b and c presents a XRD pattern of HFs and thermo gravimetric analysis (TGA) of HFs. According to TGA analysis, it is seen that the total weight loss up to 1000 °C is approximately 96.6%. The remaining ash amount after combustion is 3.4%. Combustion reaction occurred between 200 and 500 °C. The first major weight loss was observed between 200 and 380 °C and the second significant weight loss between 380 and 500 °C. Accordingly, the first rapid burning reaction can be

Table 1
Characteristics of PC.

Oxides	CaO	SiO_2	Al_2O_3	Fe_2O_3	MgO	SO_3	Na_2O	K_2O	LOI
(%)	63.48	18.93	5.22	3.42	1.76	2.69	0.45	0.71	3.17
Specific weight (g/cm^3) 3.14			Specific surface (cm^2/g) 3400			Setting time initial/final (min.)			165/210
Compressive strength (MPa) (at 2 days)					28.9				
Compressive strength (MPa) (28 days)					51.1				

Table 2
Chemical and physical characteristics of FA.

Oxides	CaO	SiO_2	Al_2O_3	Fe_2O_3	MgO	SO_3	Na_2O	K_2O	Loss in ignition
(%)	3.86	50.04	28.13	9.48	1.32	0.36	0.25	0.39	1.5
Specific weight (g/cm^3)	2.41	Finenes (cm^2/g)				2750	Color		Brown

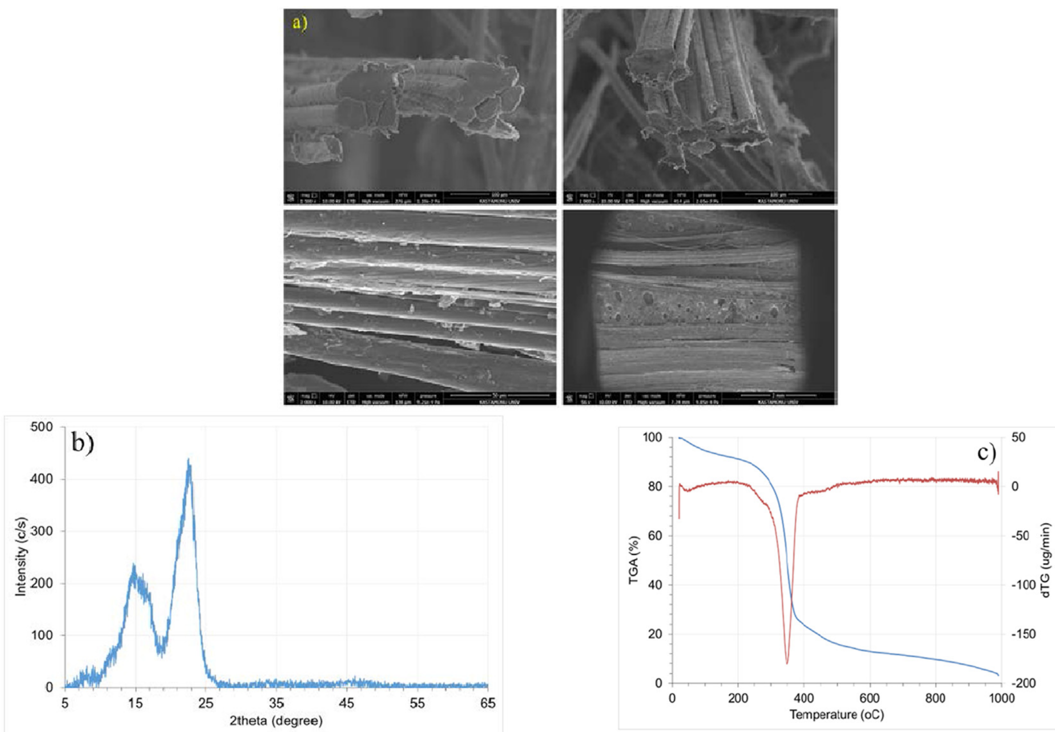

Fig. 1. a) SEM views of HFs, b) XRD pattern of HFs and c) TGA analysis of HFs.

interpreted as the burning of cellulose, which is one of the components that make up the hemp fibers, and the second slow burning reaction as lignin burning. XRD analysis 15 and 23 2theta degree peaks show characteristic peaks of cellulose.

2.1.4. Foaming agent (F)

The foaming agent contained enzyme-based proteins having 1.03 kg/l was utilized to produce concrete mixtures. Table 3 illustrates the physical properties of the agent.

Table 3
Properties of the foaming agent.

Chemical Contents	Synthetic liquid air-entraining
Appearance-Color	Translucent. pale brown liquid
Density	1.03 ± 0.02 kg/l.
pH Value	5.0 ± 1
Chloride	< % 0.1
Alkali	< % 5
Freezing	− 5 °C

2.1.5. Silica sand

Silica aggregate is used in the mortar mixtures. Its specific gravity is 2.62 and water absorption is 0.98%. The grain size is under 800 μm. D50 and D90 are about 23.8 μm and under about 227.5 μm respectively.

2.2. Mixture proportions and specimen preparation

The PC was replaced with FA at 10, 20, 30, 40 and 50% by weight. A total of 450 kg/m^3 binder and w/b ratio of 0.5 were utilized in the mixture design of foam concretes as shown in Table 4. Cement, FA, silica sand and HFs were stirred during 1 min. Water was put in and stirred for a further 2.5 min to obtain slurry paste. Foaming agent was then incorporated into slurry paste and after 2.5 min of mixing to get plastic foam concrete. To carry out the relevant tests, fresh foam concrete mix was cast in the mould. Concretes were demoulded and allowed to cure in 20 °C water during 28 days after 24 h.

Table 4
Mixture desings*.

Code	FA (%)	Foamcontent (kg/m^3)	Fiberlength (cm)	FiberRatio (%)	OPC(kg/m^3)	FA(kg/m^3)	Silica sand(kg/m^3)	Water(kg/m^3)	Fibers(kg/m^3)	w/b
R50	0	50	–	–	450	–	1204	225	–	0.5
FA0F50	0		0.5	0.75	450	0	1204	225	3.375	0.5
FA10F50	10		0.5	1.5	405	45	1191	225	6.75	0.5
FA20F50	20		1	0.75	360	90	1178	225	3.375	0.5
FA30F50	30		2	3	315	135	1165	225	13.5	0.5
FA40F50	40		1	3	270	180	1152	225	13.5	0.5
FA50F50	50		2	1.5	225	225	1139	225	6.75	0.5
R75	0	75	–	–	450	–	988	225	–	0.5
FA0F75	0		1	1.5	450	0	988	225	6.75	0.5
FA10F75	10		1	3	405	45	975	225	13.5	0.5
FA20F75	20		2	1.5	360	90	961	225	6.75	0.5
FA30F75	30		0.5	0.75	315	135	948	225	3.375	0.5
FA40F75	40		2	0.75	270	180	935	225	3.375	0.5
FA50F75	50		0.5	3	225	225	922	225	13.5	0.5
R100	0	100	–	–	450	–	771	225	–	0.5
FA0F100	0		2	3	450	0	771	225	13.5	0.5
FA10F100	10		2	0.75	405	45	758	225	3.375	0.5
FA20F100	20		0.5	3	360	90	745	225	13.5	0.5
FA30F100	30		1	1.5	315	135	732	225	6.75	0.5
FA40F100	40		0.5	1.5	270	180	718	225	6.75	0.5
FA50F100	50		1	0.75	225	225	705	225	3.375	0.5

* Mix ID such as FA10F50 means: 10% FA/fly ash and F/foam content 50 kg/m^3

2.3. Testing procedures

Slump test was done to observe workability of fresh concretes as per ASTM C1437-15 [48]. Transport properties of foamed concretes including dry unit weight, water absorption and porosity after 90 days were evaluated on the samples in 50 × 50 × 50 mm by ASTM C642 [49]. In accordance with ASTM C348-19 [50], using specimens with 40 × 40 × 160 mm size, flexural strength test was done on three samples for each mixture with 50 N/s speed. Three samples were used to take the average. To assess the compressive strength, a total of six specimens obtained after the flexural test were used to perform the tests as per ASTM C349-18 [51]. Six samples were used to take the average. Sorptivity of foam concretes was evaluated on 50 × 50 × 50 mm samples according to ASTM C1585-20 [52]. As per ASTM D7984-16 [53], the specimens of 20 × 50 × 100 mm size were utilized to measure thermal conductivity of concretes. To ASTM C 596 [54], the samples of 25 × 25 × 285 mm size were used to perform drying shrinkage of concretes. 40 × 40 × 160 mm sized concrete samples were subjected to fast freeze–thaw test in accordance with ASTM C666-97 [55]. All foam concrete samples were subjected to a total of 200 freeze–thaw cycles. Compressive, flexural strength, UPV and mass loss tests were performed every 100 cycles. After concretes subjected to temperature of 200, 400, 600 and 800 °C with a temperature rise of 10 °C/min., they were subjected to cooling slowly (In oven) and water cooling by spraying with room temperature water for five min. after samples subjected to high temperatures and F-T, UPV evaluation were performed to detect internal damage of concretes as per ASTM C597-02 [56].

2.3.1. Taguchi optimization

Each variable used in the study should be examined separately to determine its effects. If the experimental design is fully factorial, it is necessary to produce 162 mixtures. Due to the large number of mixtures in the study, Partial Factorial experimental design was used to save material and time. For this purpose, Taguchi optimization method was applied with the Taguchi L18 orthogonal experiment matrix. In addition, ANOVA analysis was performed to see the significance rates of variables used for the Taguchi matrix.

3. Results and discussion

3.1. Fresh concrete properties

Slump of all fresh concretes were plotted in Fig. 2. Slump values raised with increment of foam rate from 50 to 100 kg/m^3 due to decreasing solid content. Reference mixtures (R50, R75 and R100) generally had the highest slump of 21.5 cm, 25.6 cm and 27.7 cm in each foam content group respectively. The slump of all fresh concretes with foam of 50 kg/m^3 were in the range of 21.4 cm and 11.5 cm. The mixtures containing 30 and 40% FA and 3% HFs with fiber length of 2 cm and 1 cm (FA30F50, FA40F50) showed the lowest slump of 15.5 cm and 12.8 cm respectively. With increasing F content, the mixtures revealed higher slump values due to decreasing solid content. Replacing fly ash with ordinary Portland cement enhanced slump flow diameter

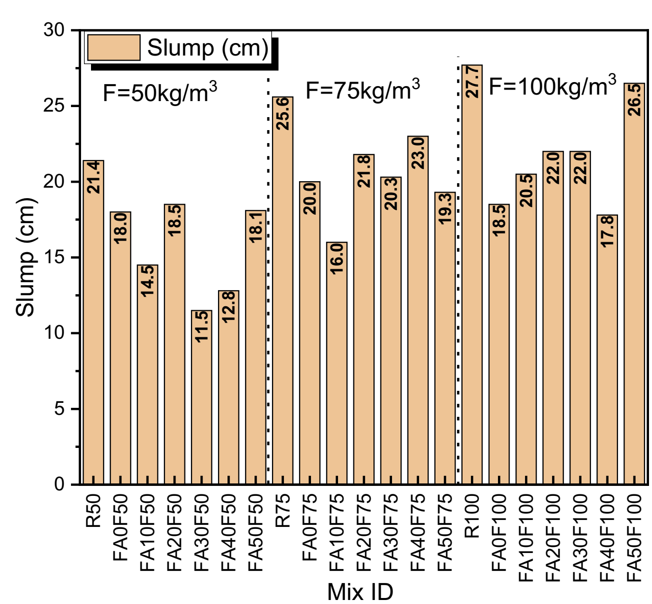

Fig. 2. Slump of concretes at F content of 50, 75 and 100 kg/m^3.

because of small round-shape and smooth texture of the FA grains [57] while inclusion of HFs had a negative impact on the slump due to the increase in water absorption amount with HFs content[28]. The slump of all fresh concretes with foam of 75 kg/m^3 were in the range of 25.6 cm and 16 cm. For the F content of 75 kg/m^3, the negative impact of HFs on the slump were seen in the mixtures containing 3% HFs with 1 cm and 0.5 fiber length; the mixtures FA10F75 and FA50F75 showed the lowest slump due to the higher HFs ratio of 3% with 1 cm and 0.5 fiber length - despite the lowest and highest FA content. The slump of all fresh concretes with F rate as 100 kg/m^3 were between 27.7 and 17.8 cm. Mixture FA50F100 containing 50% FA with 0.75% HFs provides the highest slump while FA0F100 containing 3% HFs with 2 cm length has the lowest slump value at the F content of 100 kg/m^3. It can be also concluded that increment in fiber length had negative effect on the slump values. Ruano et al. [30] pointed out that HFs actively interact with the fresh mortar and reduce the workability by taking water from the fresh mixture and changing the hydration development of cement paste. Literature includes many studies examining rheology of foam concrete - studied by viscometry. Viscosity values increase as foam content increases in foam concrete production [58–61]. As a result of the increase in cement content in the mixture, the viscosity values decrease [62]. Benli et al. [62] have shown that increment of cement dosage in mixture affected viscosity values decreasing. She et al. [14] has shown that workability increases when coarse ash is used in foam concrete. Yang et al. [63] used waste brick powder (WBP) instead of cement and reported that the workability was affected as the WBP content increased. The use of fibers in foam concrete reduces workability, but it is a very important component for crack control [64].

3.2. Compressive strength

Fig. 3 plots compressive strength of 7, 28 and 91- day concretes with F contents of 50, 75 and 100 kg/m^3. As observed for all mixes, values raised with the increment in curing age. Also increment of F volume presents a significant compressive strength reduction in Fig. 3a-c. The strength ratios for all concretes containing 50 kg/m^3 F are higher than for concretes containing 75 and 100 kg/m^3 F; there are two exceptions: the mixtures without FA (FA0F75 and FA0F100) at all curing ages. These important compressive strength reduction may be related with low solid content and negative effect of FA because of its slow pozzolanic properties [65]. Fig. 3a shows the strengths of concretes with 50 kg/m^3 F. At 7 days, with increasing F, lower strength of concretes with FA is seen than in reference mixture (R50). Also at 7 days, concrete having 0.75% HFs and no FA (FA0F50) has the highest strength (18.89 MPa). 10% compressive strength enhancement was obtained due to 0.75% HFs when compared to R50. Concrete containing 30% FA and 3% HFs with 2 cm length (FA30F50) shows 14.67% strength decrease when compared to R50. The strength of FA10F50 is nearly the same as for R50. Strength of 28-days specimen with F content of 50 kg/m^{3}varies between 8.67 and 21.34 MPa. The lowest compressive strength is seen for the FA50F50 specimen and the highest for FA30F50. At 28 days, the mixtures FA0F50 (0.75% HFs with 0.5 cm length), FA10F50 (1.5% HFs with 0.5 cm length) and FA30F50 (3% HFs with 2 cm length) have the compressive strength 9.19%, 2.65% and 10.79% higher than R50. We find that replacing cement with FA reduces the compressive strength but inclusion of HFs enhances it remarkably. The compressive strength of 91-days specimens was between 14.98 and 27.01 MPa for 50 kg/m^3 F. All mixtures show greater compressive strength values than R50, except for FA50F50. The increment of FA reduces strength because of incomplete pozzolanic reaction in which the growth of the CSH (calcium silicate hydrate) gel was slowed down by aluminum and silicon ions in FA [66]. Fig. 3b exhibits the strength of

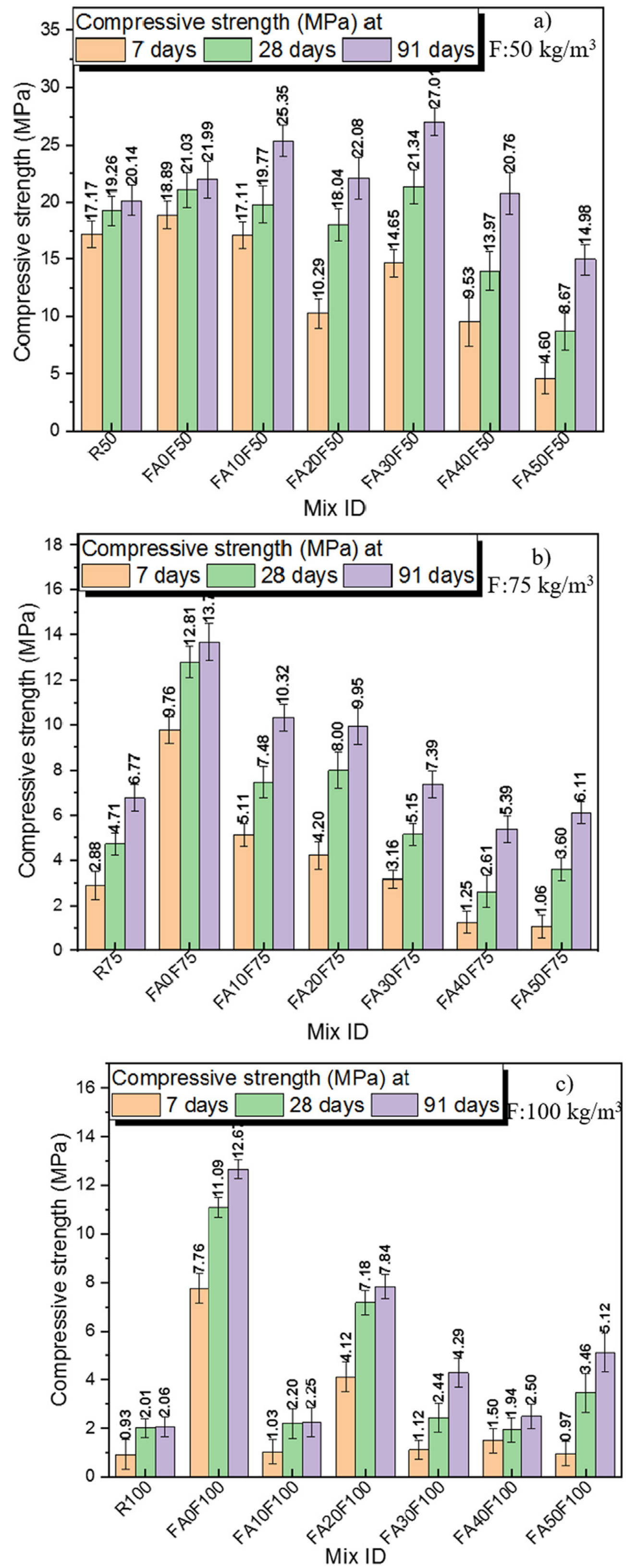

Fig. 3. Compressive strengths of foam concretes.

mixes having 75 kg/m^3 F. Actually FA0F75 (1.5% HFs, 1 cm length) gained the highest compressive strength of 9.76, 12.81 and 13.70 MPa. The mixtures incorporating 10, 20 and 30% FA gained higher strength than R75 at 7 days. The effect of HFs on strength was obviously seen at 75 kg/m^3 F. Similar strength results were seen on 28 aged- concrete mixtures. The mixtures FA10F75, FA20F75 and FA30F75 gained compressive strength enhancements by 58.81%, 69.85% and 9.34% and FA40F75 and FA50F75 had compressive strength decrease by 44.58% and 23.56% respectively compared to R75 at 28-days. At 91-days, strength enhancements in comparison with R75 specimens were 52.43%, 46.97% and 9.15% for FA10F75, FA20F75 and FA30F75 mixtures respectively. Compressive strength of FA40F75 and FA50F75 reduced by 20.38 and 9.75% compared to R75 specimens respectively. Fig. 3c plots strength of mixes with 100 kg/m^3 F. Actually FA0F100 mixture (3% HFs, 2 cm length) gained the highest compressive strength of 7.76, 11.09 and 12.67 MPa which were 7.34, 10.92 and 12.62 times higher than R100 at 7, 28 and 91 days respectively. At 28 days of curing, mixtures FA10F100, FA20F100, FA30F100 and FA50F100 gained compressive strength enhancements by 9.45%. 257.21%, 21.39% and 72.13% and FA40F100 had compressive strength decrease by 3.48% respectively compared to R100 at 28 days. All 91 aged foam concrete specimens showed higher compressive strength than reference R100 specimens. At 91 days, strength enhancements in comparison with R100 specimens were 9.22%. 280.58%, 108.25%, 21.35% and 148.54% for FA10F100, FA20F100, FA30F100, FA40F100 and FA50F100 mixtures respectively.

3.3. Flexural strength

Fig. 4 plots average flexural strength of 7, 28, and 91- day concretes. Flexural strength decreases with increasing F due to decreasing solid content and increasing porosity. The results indicated that flexural strength values strongly depended on the HFs ratio and FA content. With high HFs ratio and low FA content, higher flexural strength was obtained. The foam concretes exhibited low early-age flexural strength with increasing FA content as reported in the literature. Fig. 4a plots the flexural strength results of foam concretes with F contents of 50 kg/m^3. As expected, at 7 days curing, the mixture FA0F50 without FA and 0.75% HFs gained the highest early-age flexural strength of 3.65 MPa which was 37.73% higher than R50. This can be attributed to the that mixture without FA and high tensile strength properties of HFs [31]. After 28 days, the highest strength was observed as 4.52 MPa, 40.37% higher than R50 for the mixture FA10F50. Flexural strength enhancements of the mixtures FA0F50, FA30F50 and FA40F50 compared to R50 specimens were 16%, 27.95% and 4.96% respectively. Although FA30F50 and FA40F50 had the same HFs ratio of 3% but the different length of 2 cm and 1 cm, the increment in the flexural strength between them was 5.6 times higher. FA50F50 exhibited the lowest early 28- aged flexural strength of 2.41 MPa. After 91 days curing, all mixtures revealed higher flexural strength than reference concrete R50 and the mixture FA10F50 shown the highest flexural strength (5.88 MPa), 69.94% higher than R50. Fig. 4b plots the flexural strength results of foam concrete with 75 kg/m^3 F. Lower flexural strength rates when compared to mixes having 50 kg/m^3 F were obtained because of low solid amount and higher porosity. At early 7- age of curing, the mixtures containing FA content between 0 and 30 percent showed higher flexural strength than reference R75. FA10F75 with 3% HFs, 1 cm length, performed the best flexural performance at all curing ages with the flexural strength increase of 240.54%, 354.05% and 395.94% aged 7, 28 and 91 days respectively. FA0F75, FA20F75 and FA30F75 had also higher flexural strength than R75 with strength increase of 200%, 130.55%, 71.17% and 228.37%, 150%, 84.11% and 28.37%, 16.66% and 15.88% aged 7, 28 and 91 days respectively. Although the mixtures FA40F75 and FA50F75 had lower flexural strength than R75 at 7 days, they revealed higher flexural strength than R75 after 28 and 91 days. Fig. 4c depicts the flexural strength results of concretes with F contents of

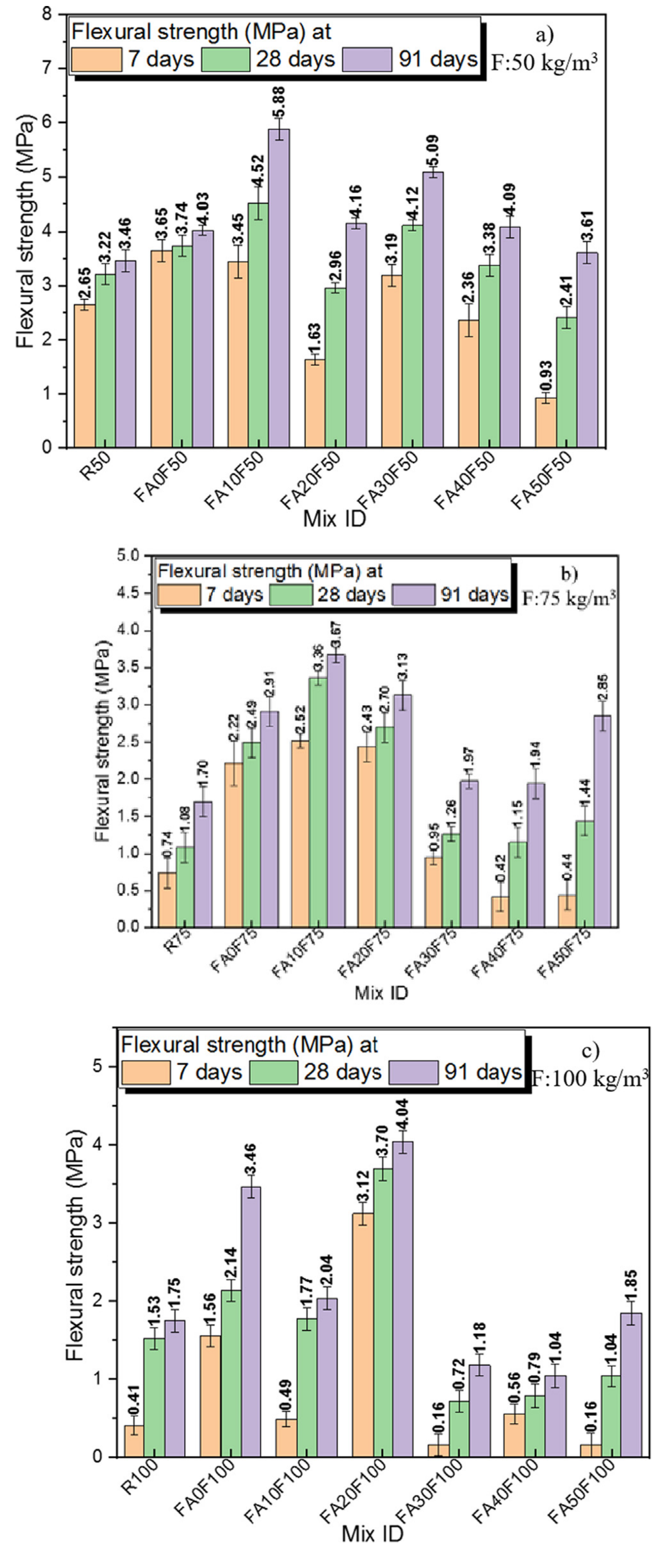

Fig. 4. Flexural strengths of foam concretes.

100 kg/m^3. The mixtures FA0F100 and FA20F100 with 3% HFs content revealed the highest 7, 28 and 91 aged strengths. Mixture FA20F100 with fiber length of 0.5 cm performed better than the mixture FA0F100 with fiber length of 2 cm. This means that the mixtures containing short fiber length with the same HFs ratio showed better performance. Similar flexural strength performance was also observed for the mixtures FA30F100 and FA40F100 con-

taining the same HFs ratio of 1.5% with the length of 1 cm and 0.5 cm respectively. Although FA40F100 had higher FA content, its flexural strength was bigger than FA30F100 at 7 and 28 days. This is because of short HFs length of FA40F100. Flexural strength enhancements for the mixtures FA0F100 and FA20F100 compared to R100 aged 7, 28 and 91 days were 280.48%, 39.86%, 97.71% and 660.97%. 141.83% and 130.85% respectively.

3.4. Dry unit weight and thermal conductivity

Fig. 5 plots dry unit weight and thermal conductivity results of 28 aged concretes. The unit weight outcomes are shown in Fig. 5a. Unit weights of foam concretes reduced with increasing foam and FA due to decreasing solid content and lower specific gravity of FA than cement [67]. Effect of HFs on the dry unit weight has presented that the fiber addition causes dry unit weight enhancement in some mixtures having 50 kg/m^3 F. Dry unit weights of the mixes having 75 and 100 kg/m^3 F generally reduced with HFs content and increasing FA content. Reference concretes R75 and R100 showed the highest unit weight in the mixtures with 75 kg/m^3 F and 100 kg/m^3 F. Concretes with 50 kg/m^3 F exhibited higher unit weight than R50 except the mixes FA20F50 and FA50F50. With 5.8% increase compared to R50. FA30F50 had the highest unit weight and FA50F50 had the lowest unit weight and revealed 7.11% decrease in unit weight compared to R50. As mentioned before, R75 had the highest unit weight and FA40F75 showed the lowest unit weight with 24.69% decrease compared to R75. FA30R75 had the lowest unit weight reduction of 1% compared to R75. Reference concrete R100 had the highest unit weight and FA30F100 showed the lowest unit weight with 30.62% decrease compared to R100. FA0R100 had the lowest unit weight reduction of 0.71% compared to reference specimen R100.

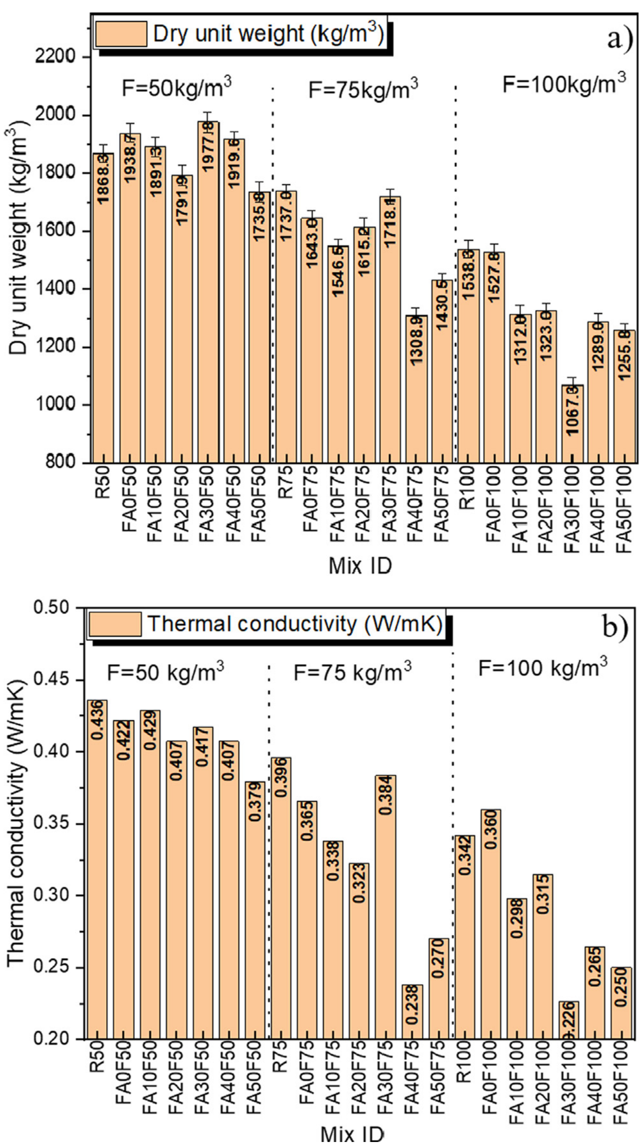

Fig. 5. a) Dry unit weights and b) Thermal conductivities of foam concretes.

Fig. 5b plots thermal conductivity results of foam concretes with 50, 75 and 100 kg/m^3 F. Thermal conductivity of concretes reduced as foam and FA content increased due to decreasing solid content and increasing porosity. A decrease in the thermal conductivity was also observed at HFs content of 0.75 and 1.5% but a slight thermal conductivity increase was seen at HFs ratio of 3%. Mixes having 50 kg/m^3 F exhibited less thermal conductivity values than reference R50. FA50F50 presented the lowest value (0.379 W/mK) that was 13.07% lower than reference R50. Since the unit weight and porosity of concretes affect the thermal conductivity strongly, lower unit weight leads to greater porosity and less thermal conductivity. Since replacing cement with FA decreased the unit weight of foam concrete. This caused the greater porosity and less thermal conductivity [68]. The results indicated that mixes having 75 kg/m^3 F presented less conductivity values than reference R75. FA40F75 revealed the lowest conductivity rate (0.238 W/mK) that was 39.89% lower than reference R75. The thermal conductivity reductions of 7.82%, 14.64%, 18.43%, 3.03% and 31.81% were obtained for the mixtures FA0F75, FA10F75, FA20F75, FA30F75 and FA50F75 compared to R75. In F content of 100 kg/m^3, the results presented that all mixtures presented lower thermal conductivity values than reference R100 except FA0F100 which was 2.26% higher than R75. FA30F100 showed the lowest conductivity value (0.226 W/mK) that was 33.91% lower than reference R100. The thermal conductivity reductions of 12.86%, 7.89%, 22.51% and 26.90% were obtained for the mixtures FA10F100, FA20F100, FA40F100 and FA50F100 compared to R100 respectively. It can be concluded that the lowest thermal conductivity changed depending on FA content. 50% FA, 40% FA and 30% FA were the optimum contents for lower thermal conductively at 50, 75 and 100 kg/m^3 F, respectively.

3.5. Porosity and water absorption

Fig. 6a-b plots the unit weight, porosity and water absorption of concretes. Fig. 6a depicts the relation between porosity and absorption. As shown from Fig. 6a, with increasing F content, water absorption and porosity also increased due to decreasing solid content of mixtures. At low content of FA, water absorption and porosity tended to decrease but increase after 30% FA content because of slow pozzolanic activity of FA and dilution influence of cement [36,37]. HFs content affected the water absorption and porosity of concretes positively at low FA or without FA content and negatively with high FA content. The reference concrete R50 had the lowest absorption and porosity FA50F50 exhibited the highest porosity and absorption with an increase of 40.52% and 66.36% compared to R50 respectively at 50 kg/m^3 F. FA30F75 presented the lowest porosity and absorption with decreases of 1.91% and 9.67% compared to R75 and FA0F75 had the highest porosity and absorption with increases 85.52% and 125.99% compared to R75 respectively at 75 kg/m^3 F. At 100 kg/m^3 F, FA0F100 presented the lowest porosity and absorption with decreases of 19.22% and 26.75% compared to R100 and FA30F100 had the highest porosity and water absorption with increases 71.15% and 105.93% against R100 respectively. Fig. 6b shown relation between porosity and

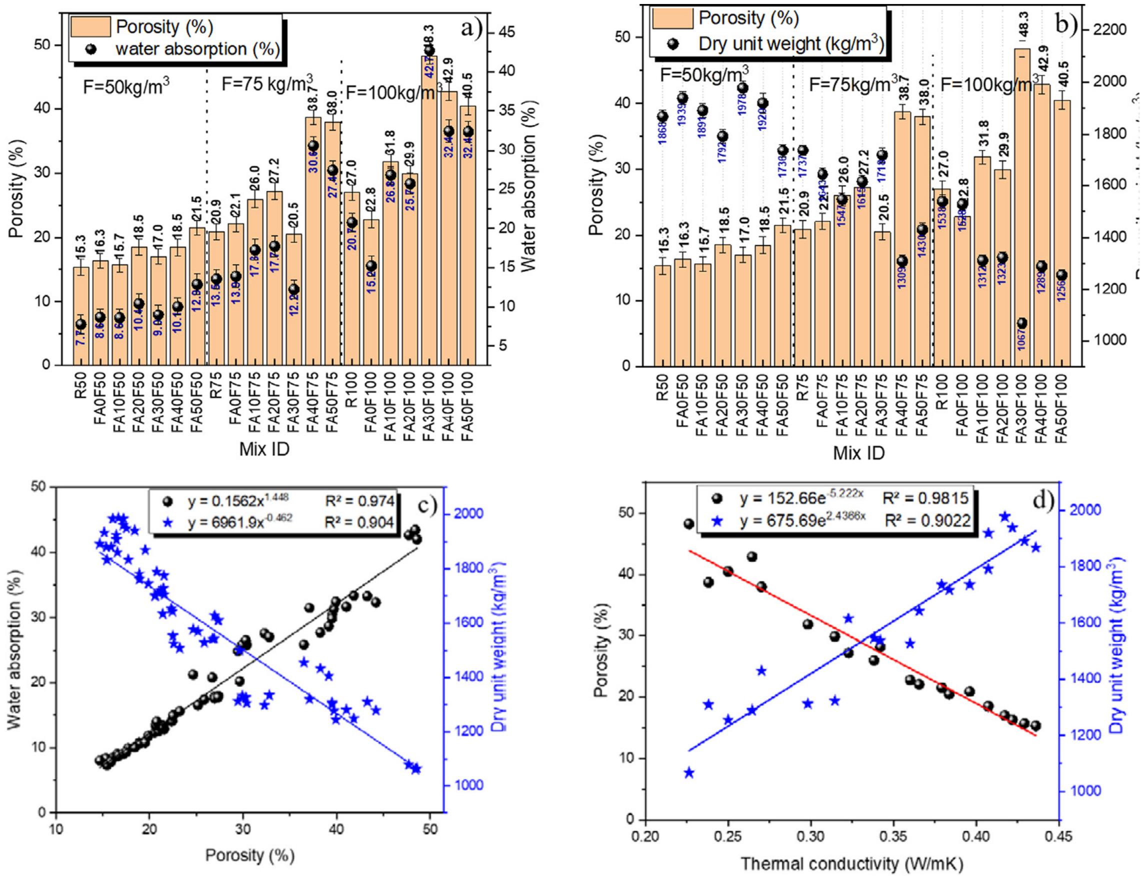

Fig. 6. a) Porosity vs. water absorption, b) Porosity vs. dry unit weight results, c) Porosity vs. water absorption and dry unit weight, b) thermal conductivity vs. porosity and dry unit weight.

dry unit weight. As illustrated in Fig. 6b, with increasing foam content, porosity increased and dry unit weight decreased due to decreasing solid content of mixtures. Very good relation between porosity and dry unit weight was clearly observed. At high content of FA, the mixtures generally had higher dry unit weight with increasing HFs content at 50 kg/m^3 F. At 75 and 100 kg/m^3 F, with decreasing solid content, reference concretes R75 and R100 exhibited the highest unit weight with increasing FA content because of less specific gravity of FA than cement.

Fig. 6c-d shows the link among the porosity and absorption and dry unit weight of foam concretes and Fig. 6d illustrates the thermal conductivity and porosity and unit weight. Because absorption and unit weight strongly depends on porosity, very strong relation between the porosity vs. absorption and porosity and dry unit weight were established with 0.97 and 0.90 coefficients of correlation respectively. Because thermal conductivity is highly related with porosity and unit weight of concrete. A very effective link was also established among the thermal conductivity vs. porosity and thermal conductivity vs. unit weight as 0.98 and 0.90 correlation.

3.6. Drying shrinkage

Drying shrinkage up to 120 days at different ages for different concretes is shown in Fig. 7. Obviously, mixtures presented a high strain at an early age when compared to lately shrinkage. Dry shrinkage rates grew dramatically during the first 7 days at 50, 75 and 100 kg/m^3 F. In Fig. 7a-c, higher foam content led to higher drying shrinkage due to decreasing solid content and FA inclusion reduced the shrinkage significantly and the mixtures containing 50% FA had the lowest shrinkage at 120 days in all foam contents. HFs affected the drying shrinkage positively more especially at low foam content and it seems HFs reduced drying shrinkage slightly at high foam contents. Many studies proved that replacing cement with FA reduced the drying shrinkage [69–72]. The reason for the reduction in the dry shrinkage is because of reaction that FA consumes more free water, departing less water to evaporate and thus less shrinkage. Reduction in evaporation because of capillarity while drying due to enhancement in the pore structure of concrete declines shrinkage [73]. Outcomes indicated that maximum shrinkage observed in reference concretes R50, R75 and R100 as shown in Fig. 7a-c. Fig. 7a plots drying shrinkage of concretes having 50 kg/m^3 F. After 91 days, it seems that shrinkage tended to decrease slightly until 120 days. Reference concrete R50 exhibited the highest shrinkage at all drying times and with FA inclusion rate, dry shrinkage reduced and reached the lowest values at 50% FA replacement. The dry shrinkage reduction of the mixture FA50F50 compared to R50 was 54.51%. The dry shrinkage reduction for the mixtures FA0F50, FA10F50, FA20F50, FA30F50 and FA40F50 compared to R50 was found to be 6.63%, 20.34%, 31.34%, 47.70% and 49.75%. High shrinkage reduction in the mixtures FA30F50 and FA40F50 can be due to the high HFs content of 3%. Fig. 7b presents shrinkage of concretes having 75 kg/m^3 F. Similar shrinkage behavior was observed in this foam content mixtures. The dry shrinkage reduction of 16.33%, 29.06%, 42.83%, 50.34%, 47.30% and 59.73% compared to R75 was obtained for the mixtures FA0F75, FA10F75, FA20F75, FA30F75, FA40F75 and FA50F75 respectively. The reductions at 100 kg/m^3 F were 1.23%, 18.02%, 29.03%, 36.85%, 47.90% and 51.53% for the mixtures containing FA of 0–50% respectively compared to R100. It can be con-

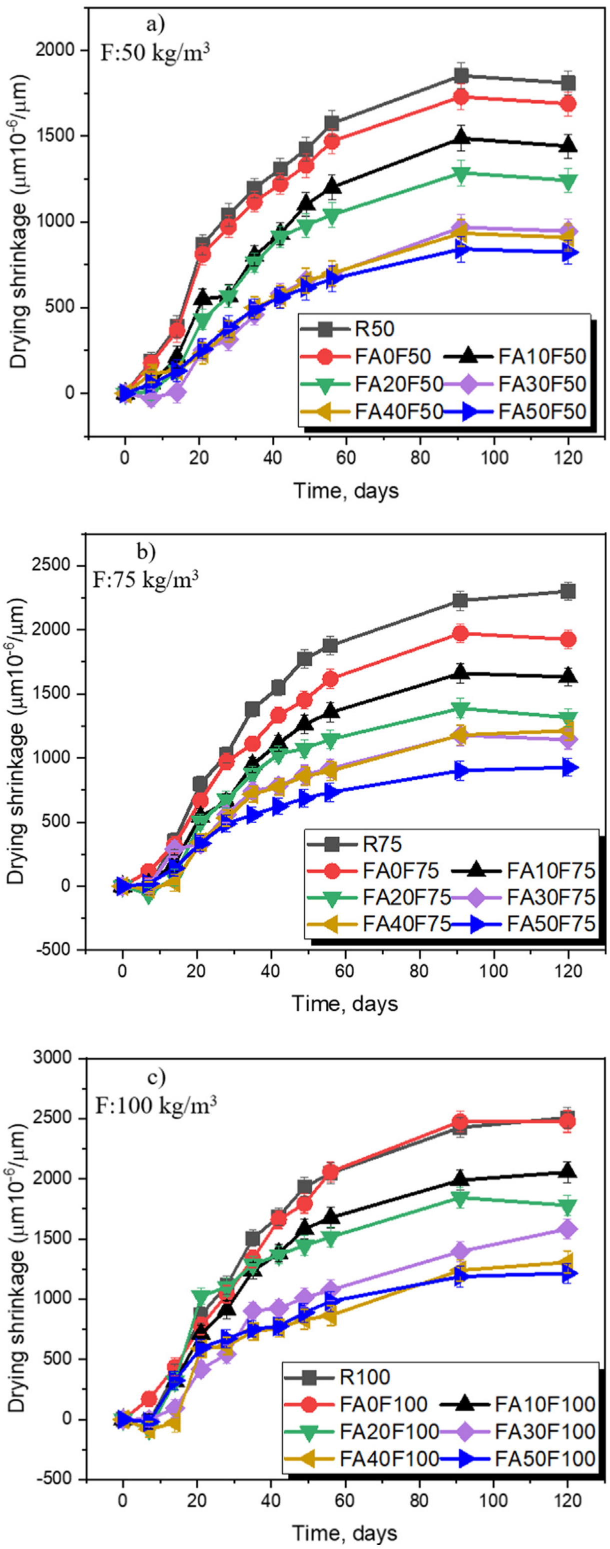

Fig. 7. Drying shrinkage values of foam concretes.

cluded from the reduction values that at 3% HFs content, dry shrinkage reduction was high in comparison with the mixtures containing low content of HFs.

3.7. Sorptivity

Fig. 8 plots sorptivity values up to 28 days of concretes. As seen in Fig. 8a-c, the sorptivity of foam concretes increased with increasing foam content due to decreasing solid content and increasing porosity. Fig. 8a presents the sorptivity of specimens having 50 kg/m^3 F. In Fig. 8a, reference mixture R50 had the lowest sorptivity values and the addition of FA increased it and reached the highest values at a replacement rate of 50% FA. Similar results was obtained by the authors [36,71,74]. After 14 days, sorptivity of the mixture FA50F50 showed a sharp increase and 46.26% enhancement in the sorptivity compared to R50 was obtained for FA50F50. The effect of HFs on the sorptivity in mixes having 50 kg/m^3 F was not clearly seen. Fig. 8b shows the sorptivity of concretes with foam of 75 kg/m^3. Influence of HFs on sorptivity was clearly seen in this foam content mixtures. After 28 days. FA10F75 with 3% HFs exhibited the lowest sorptivity with sorptivity reduction of 23.15% compared to R75 and FA50F75 with 3% HFs had also lower sorptivity than FA40F75 which had the highest sorptivity with an increase of 41.78% compared to R75. Fig. 8c plots the sorptivity of concretes with foam of 100 kg/m^3. In this foam content, impact of HFs on the sorptivity was very clear and significant. FA0F100 and FA20F100 containing 3% HFs showed lower sorptivity than all other mixtures with reduction of 45.65% and 34.45% compared to R100 respectively. FA50F100 also showed lower sorptivity with a decrease of 16.15% than R100. FA30F100 and FA40F100 with 1.5% HFs content had very higher sorptivity than R100 and FA30F100 depicted the highest sorptivity with an increase of 61.81% compared to R100. Changes in compressive strength with the sorptivity rates of 28 aged foam concretes were given in Fig. 8d. The results indicated that an inverse connection among strength and sorptivity is established as also mentioned by Kanellopoulos et al. [75]. There was a clear relation among strength and sorptivity with a 0.87 correlation ratio.

3.8. High temperature exposure

The foam concretes were firstly dried at 100 °C during 24 h, later exposed to 250, 500, 750 and 1000 °C during 2 h at 10 °C / minute heating. After subjection, concretes were subjected to air cooling.

3.8.1. Compressive strength

Fig. 9 plots compressive strength of after room and high temperature. As plotted in Fig. 9, the compressive strength of concretes performed very well and generally increased at the temperature exposure of 250 °C and 500 °C in comparison with the compressive strength at 20 °C. This enhancement was mostly endorsed because of pozzolanic reaction and rise in hydration process that produces higher density C-S-H increasing strength, as reported in the literature [22,76,77]. Many studies have also focused on mechanical and durability performance of concrete having FA [8–11] at high temperatures. In short, it has been found that FA improves concrete performance at high temperatures and the development is important at temperatures under 600 °C [78–80] which was in agreement with our results. As shown in Fig. 9, mixtures having 50 kg/m^3 F presented bigger strength at all temperature exposure than mixtures having 75 and 100 kg/m^3 F. After 750 °C, a sharp strength decrease was seen on all mixture specimens. Slightly positive impact of HFs on the strength of foam concretes subjected to high temperature was clearly seen at temperature range 250–500 °C. As shown in Fig. 9a, almost all mixtures (a small decline in FA20F50 at 500 °C) exhibited compressive strength enhancements at temperature of 250–500 °C. Percent enhancements in strength at 250 °C was 23.2%, 24.9%, 47.7%, 31.7%, 32.7%, 62.3% and 78.3% for the mixtures from R50 to FA50F50 in comparison with ambient temperature strength respectively as shown in Fig. 9a. With 62.3% and 78.3% enhancements, FA40F50 and FA50F50 presented the highest increment rate. When strength changes of two mixtures R50 and FA0FA50 without FA and latter with HFs were compared, it can

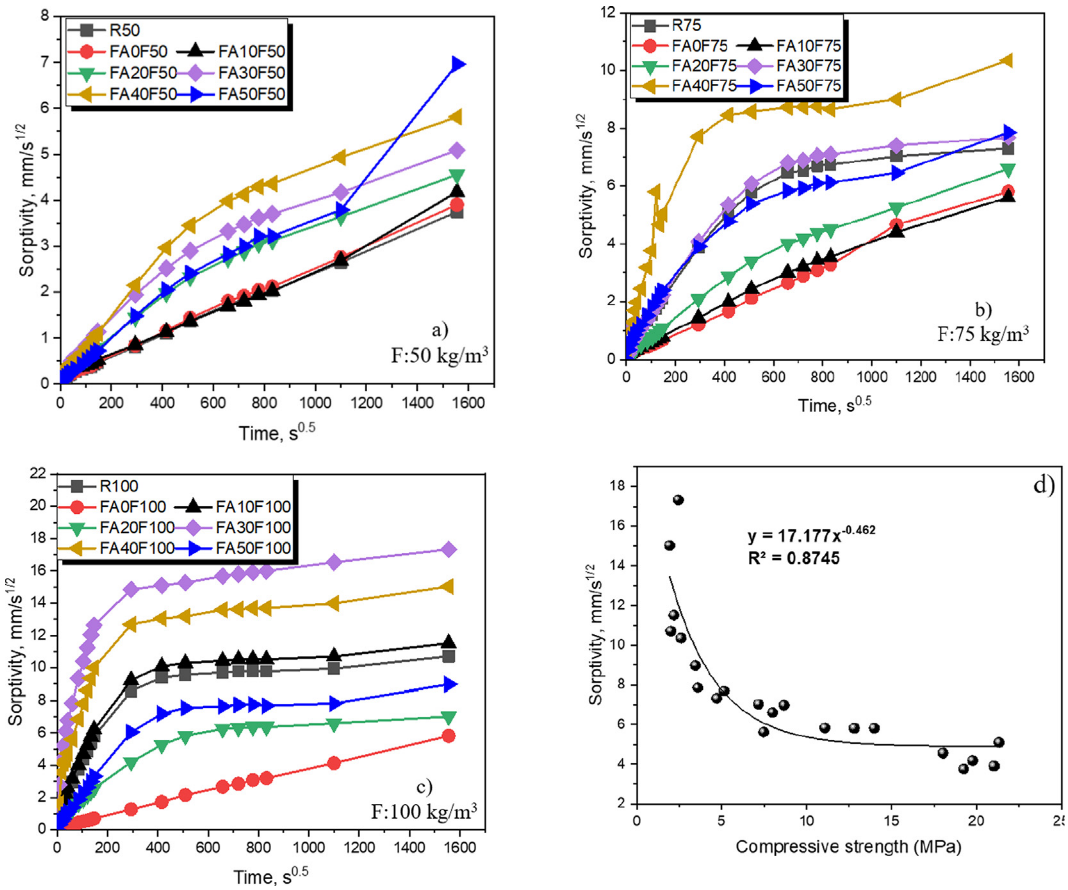

Fig. 8. Sorptivities of foam concretes, and compressive strength vs. sorptivity relation.

be noted that the mixture with HFs had higher strength increase than R50 but after 750 °C, the strength reduction of these two mixtures were nearly the same. FA10F50 and FA50F50 performed the best temperature performance at 500 °C and FA10F50 gained the highest strength at 500 °C when compared to strength at ambient temperature. At 750 °C, FA40F50 and FA50F50 exhibited the best performance with the strength reduction of 32% and 37.6% when compared to strength at ambient temperature respectively. At 1000 °C, the lowest strength losses of 65.5, 68.1 and 66.8% were obtained for the mixtures FA10F50, FA40F50 and FA50F50 in comparison with ambient temperature strength. Fig. 9b presents the variation of strength of mix having 75 kg/m^3 F. All mixtures in this foam content exhibited strength increases at 250 °C and percent enhancements in strength at 250 °C were 17%, 32.9%, 58.8%, 36.8%, 20.4%, 93.5% and 33.1% for the mixtures from R75 to FA50F75 in comparison with ambient temperature strength respectively. It can be reported that the mixture containing 40% FA (FA40F75) showed the best performance at all temperature exposure ranges with increases of 93.5% and 236.1% at 250 °C and 500 °C respectively and reductions of 34.1% and 64.0% at 750 °C and 1000 °C respectively. Percent reductions of other mixtures in strength at 750 °C and 1000 °C were between 60 and 66% and 75–84% respectively. Fig. 9c presents the change in strength of mixes having 100 kg/m^3 F. All mixtures in this foam content revealed strength enhancements at 250 °C and percent enhancements in strength were 18.9%, 23.3%, 21.9%, 8.9%, 2.9%, 70.5% and 23.4% for the mixtures from R100 to FA50F100 in comparison with ambient temperature strength respectively. Mixture having 40% FA (FA40F100) performed the best resistance at all temperature exposure ranges with increases of 70.5% and 81.86% at 250 °C and 500 °C respectively and reductions of 57.5% and 66.8% at 750 °C and 1000 °C respectively. Percent reductions of other mixtures in strength at 750 °C and 1000 °C were between 70 and 85.2% and 72–88% respectively. The mixtures containing 40% FA with foam content of 75 and 100 kg/m^3 performed best resistance to all high temperature ranges. It can be concluded that optimum FA content was 40% as also pointed out by Rais et al. [81].

3.8.2. Flexural strength

Fig. 10 plots flexural strength of concretes. Foam concretes exposed to elevated temperatures exhibited higher flexural strength decrease than compressive strength because of micro cracks and increasing of brittleness; this became a serious danger when samples were exposed to tensile stress. As seen in Fig. 10, all mixture specimens lost their strength completely at 1000 °C. An interesting result was that some mixtures had higher strength reduction at 250 °C than that at 500 °C. The inclusion of HFs also affected the flexural strength positively. As foam content increases, the strength reduction of all mixture specimens increased due to the decreasing solid content and increase in the porosity. It is clearly observed in Fig. 10, all concretes had reduced the flexural strength at all temperature ranges except the concretes FA30F50 and FA0F100 which had enhancements of 0.24% and 12.6% at 500 °C in comparison with ambient temperature strength respectively. According to the relevant literature [82–84], this significant strength decrease may be because of decomposition of calcium hydroxide getting matrix cracked. With rising temperature, strength of foam concrete samples continues to decrease significantly. Fig. 10a plots the flexural strength variations of 28-aged concretes having 50 kg/m^3 F after 250–1000 °C. FA20F50 exhibited

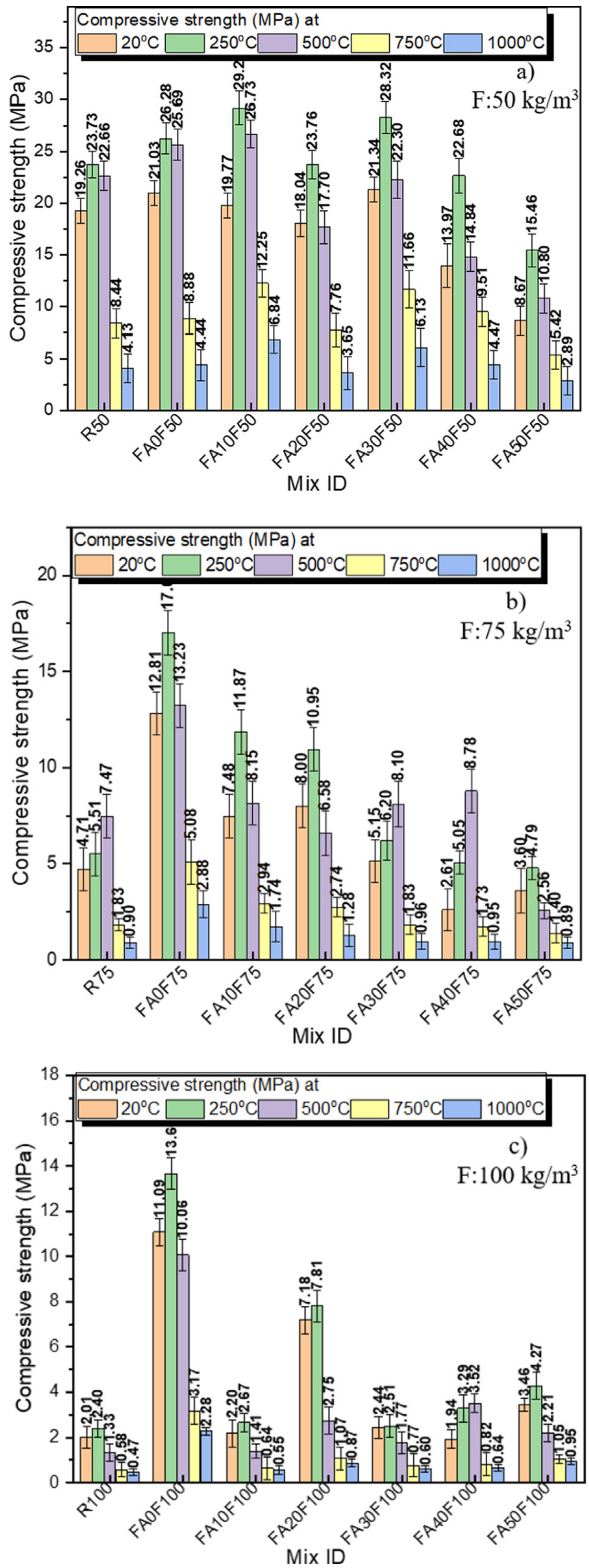

Fig. 9. Compressive strengths of foam concretes.

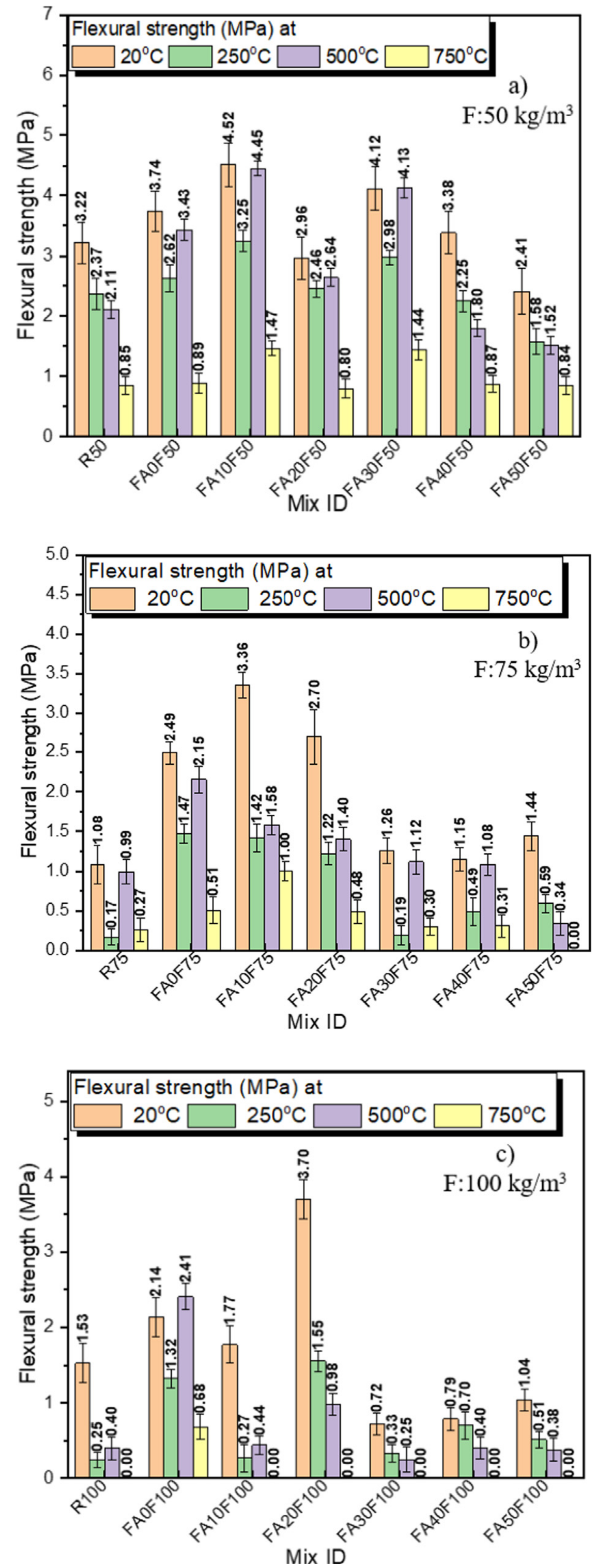

Fig. 10. Flexural strengths of foam concretes.

the lowest strength reduction of 17.2% and FA50F50 had the highest strength reduction of 34.4% at 250 °C. At 500 °C and 750 °C, FA30F50 showed the best temperature resistance with an enhancement of 0.24% and a reduction of 65% respectively. Fig. 10b plots the flexural strength variations of 28-aged concretes having 75 kg/m^3 F after 250–1000 °C. FA0F75 exhibited the lowest strength reduction of 41% and FA30F75 had the highest strength reduction of 84.9% at 250 °C. At 500 °C, R75 exhibited the best temperature resistance with a decrease of 1.0%. At 750 °C, FA10F75 illustrated the best temperature resistance with a reduction of 70.5%. Fig. 10c introduces the strength variations of concretes having 100 kg/m^3 F at 250–1000 °C. Strength reduction was higher than that of the mixtures containing 50 and 75 kg/m^3 F. FA40F100 revealed the lowest strength reduction of 11.4% and FA10F100 showed the highest strength reduction of 84.7% at 250 °C. At 500 °C and 750 °C, FA0F100 showed the best high temperature performance with an increase of 12.6% and a reduction of 68.2% respectively. This may be due to the inclusion of 3% HF content.

3.8.3. Mass loss

Fig. 11 plots mass loss after exposure to different temperatures. The mass-loss rate increased as temperature and foam content increased. It also seems that inclusion of HFs generally decreased the mass loss of mixtures in comparison with ambient temperature mass. It appears that highest mass loss was 2% and most of mixture had mass loss under 1% at 250 °C. The results indicated that mass loss of mixtures were proportional with compressive strength of mixes subjected to the same temperatures. Fig. 11a presents the mass loss of the mixes containing 50 kg/m^3 F. The mass loss was in the range of 0.5–1.2% at 250 °C in comparison with ambient temperature mass. The mixtures containing 40% and 50% FA exhibited 1.2% and 1.0% mass loss which was higher than that of other mixtures respectively. FA50F50 exhibited the lowest mass loss of 3.3% and 4.8% at 500 °C and 750 °C and the highest mass loss of 4.1% was obtained for the mixtures FA10F50 and FA30F50 after 500 °C in comparison with ambient temperature mass. Reference mixture R75 showed the highest mass loss after 750 °C and the mixture FA30F50 had the lowest mass loss at 1000 °C. As shown in Fig. 11b, FA30F75 exhibited the best performance and FA10F75 had the worst performance at high temperature in terms of mass loss after 750 °C. The mixtures showed very similar mass loss values at 500 °C. As seen in Fig. 11c, FA20F100 had the lowest loss and R100 had the highest mass loss at 1000 °C. FA50F100 shown the lowest loss and FA0F100 showed the highest loss at 750 °C. FA40F100 revealed the best performance at 500 °C in comparison with ambient temperature mass.

3.8.4. Reductions in UPV

Fig. 12a-c plots the ultrasonic velocity after exposure to different temperatures. As plotted in Fig. 12a-c, UPV reductions increased as temperature increased and it seems inclusion of HFs decreased UPV reduction before the temperature exposure of 500 °C. The range of UPV reductions at 250 °C were between 3.1 and 7% for the mixtures in comparison with ambient temperature UPV values with foam of 50 kg/m^3 as plotted in Fig. 12a. FA30F50 had the lowest and R50 had the highest UPV reduction at related temperature. At 500 °C, UPV reduction ranged from 19.2 to 36.5% and the lowest reduction belonged to FA10F50 and the highest reduction belonged to FA40F50. After 750 °C, FA30F50 had the lowest UPV drop of 60.9% and R50 had the highest UPV drop of 65.9%. UPV reductions at 1000 °C were in the range of 71–74.6%. Fig. 12b presents the UPV reductions of the mixtures containing foam content of 75 kg/m^3 as compared to ambient temperature UPV values. Reference mixture R75 and FA30F75 had the same UPV reductions at all temperature ranges and the lowest UPV reductions of 13.9, 57.3 and 62.3% at 500 °C, 750 °C and 1000 °C in comparison with ambient temperature UPV values respectively. Fig. 12c presents the UPV reductions of the mixtures containing foam of 100 kg/m^3 as compared to UPV values at ambient temperature. 30% FA blended foam concretes specimens performed best performance in terms of UPV results. Fig. 12d presented relations among com-

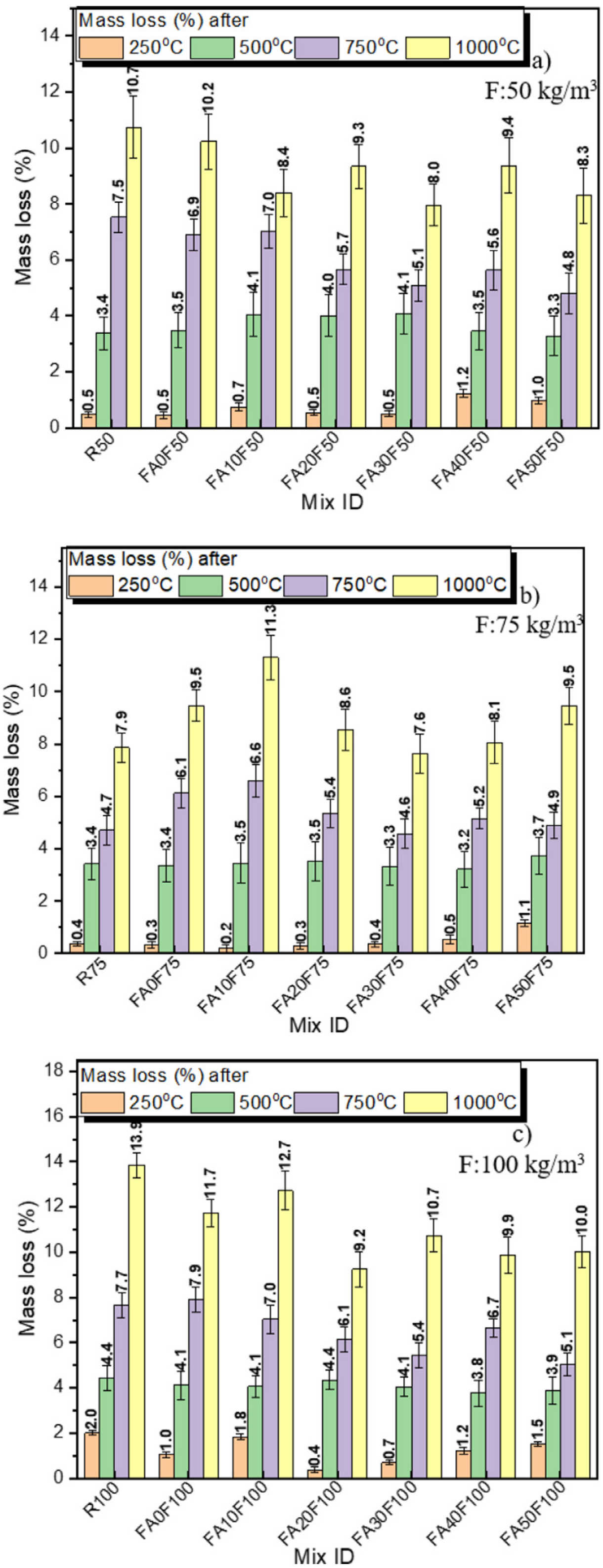

Fig. 11. Mass loss variations of foam concretes.

pressive strength and UPV of 28-aged foam concrete specimens at 20 °C, 250 °C, 500 °C, 750 °C and 1000 °C. As shown in Fig. 12d, according to the regression analysis, parabolic connection among compressive strength and UPV rates of foam concretes was supported via outcomes as 0.845, 0.908, 0.881, 0.712 and 0.777 for

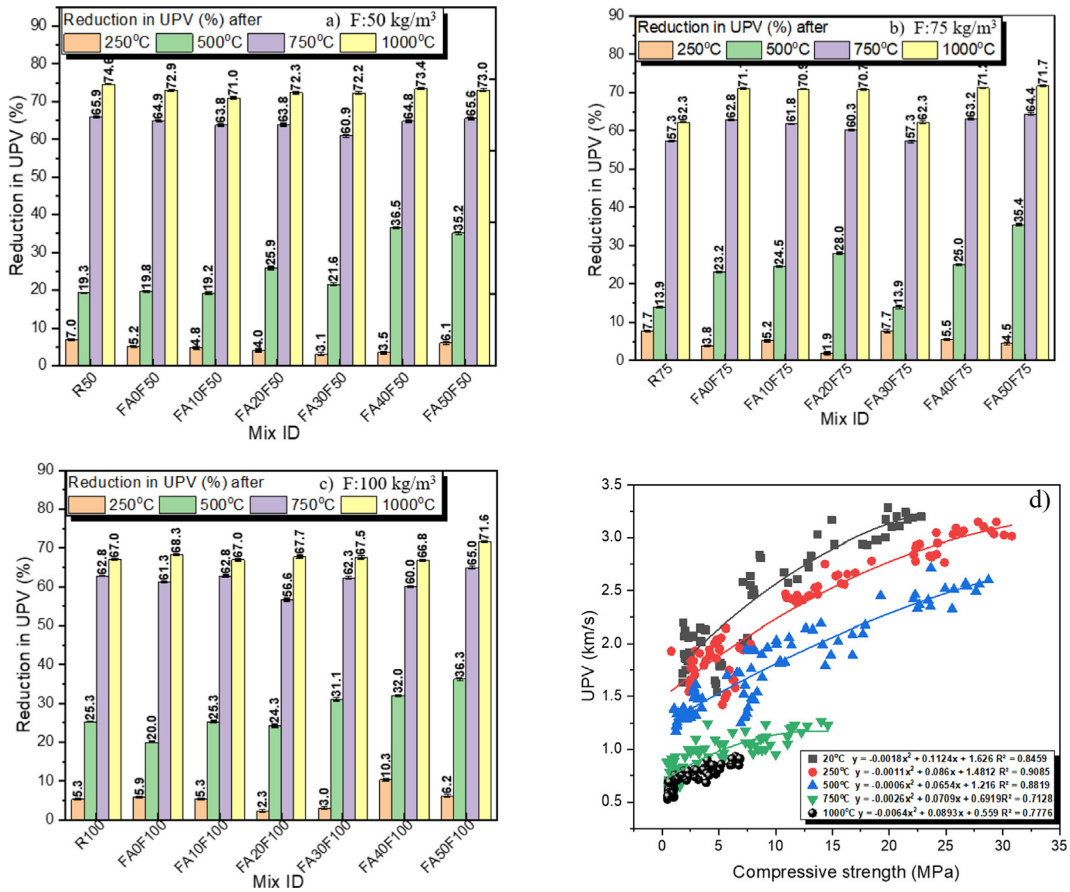

Fig. 12. Reductions in UPV of foam concretes and compressive strength vs. UPV values.

the coefficient of correlation (R^2) at 20 °C, 250 °C, 500 °C, 750 °C and 1000 °C respectively. A correlation coefficient of 0.7 or higher is considered as good score by most statisticians [85]. As per Fig. 12, lessening of compressive strength causes also reduction in the UPV values.

3.9. Freeze -Thaw (F-T) durability

3.9.1. Compressive and flexural strength

Fig. 13a plots compressive strength behind subjection to F-T. In Fig. 13a, all concretes showed that compressive strength increases behind 50F-T. Curing time of sample subjected to F-T cycles, longer than 28 days compressive strength of concretes which were not subjected to F-T resulted in increment of strength behind 50F-T as reported [86]. It seems that HFs had negative effect on the enhancement of concrete strength when compared to reference concrete and the concretes without FA. All mixtures without FA (FA0F50, FA0F75 and FA0F100) showed the lowest strength increases at all foam contents due to probably the addition of HFs. As shown in Fig. 13a, the mixtures with 40% and 50% FA (FA40F50 and FA50F50) presented the highest compressive strength enhancements as 30.3% and 52.5% respectively and the mixture without FA (FA0F50) presented the lowest strength increase. The highest strength enhancement as 119.1% was achieved for the reference concrete R75 and the lowest strength increase belonged to the mixture without FA (FA0F75). 30% FA blended concrete had the highest compressive strength increase of 109.1% and 20% FA blended concrete showed the lowest strength increase. It can be concluded that 30% FA blended foam concrete with foam of 75 kg/m^3 performed the best at F-T exposure. Very huge strength enhancement of 309.0% was observed for the reference concrete R100 with foam content of 100 kg/m^3. In this foam content, 10%FA blended concrete showed the best performance with strength increase of 106.4% and the strength enhancement decreased with increasing after 10% FA content.

Fig. 13a plots the flexural strength behind subjection to F-T cycles. In Fig. 13b, all concretes exhibited the flexural strength enhancements at all foam contents behind 50F-T cycles and all reference concretes (R50, R75 and R100) exhibited higher enhancements than foam concretes containing FA and HFs at each foam content. This means that FA and HFs affected the flexural strength positively less when concrete exposed to 50F-T cycles. As stated, R50 exhibited the highest strength increase and 30% FA blended concrete had the lowest strength increase and among FA blended concretes, 20% FA blended concretes showed the best performance., FA30F75 with foam content of 75 kg/m^{3}exhibited the highest strength enhancement among FA blended concretes and FA10F75 had the lowest strength increase. Similarly, FA30F100 exhibited the highest strength enhancement among FA blended concretes and FA20F75 had the lowest strength increase.

3.9.2. Mass loss and change in UPV

Fig. 14a plots the mass loss behind 50F-T. As plotted in Fig. 14a, the loss of all concretes decreased with increasing foam content. The mass loss was e in the range of 0.52–1.28%. It can be also concluded that mass loss decreased with increasing FA content. FA10F50 with foam content of 50 kg/m^{3}exhibited the highest loss and FA50F50 had the lowest loss. FA0F75 with foam content of 75 kg/m^{3}exhibited the highest mass loss and FA40F75 had the lowest mass loss. FA0F100 with foam content of 100 kg/m^{3}exhibited

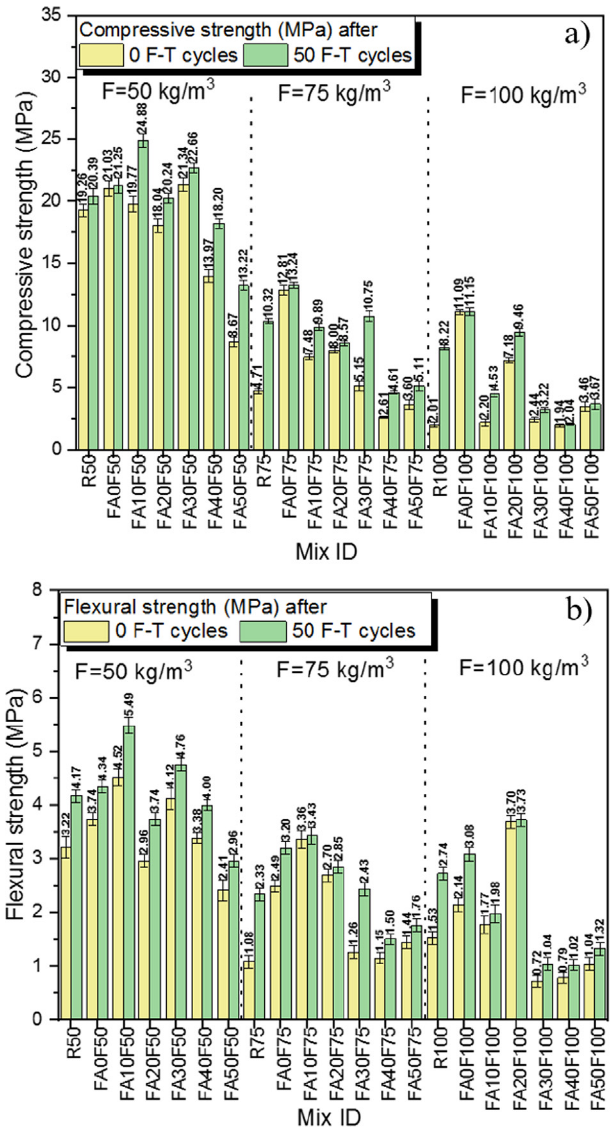

Fig. 13. a) Compressive strengths and b) Flexural strengths of foam concretes after 0 and 50F-T cycles.

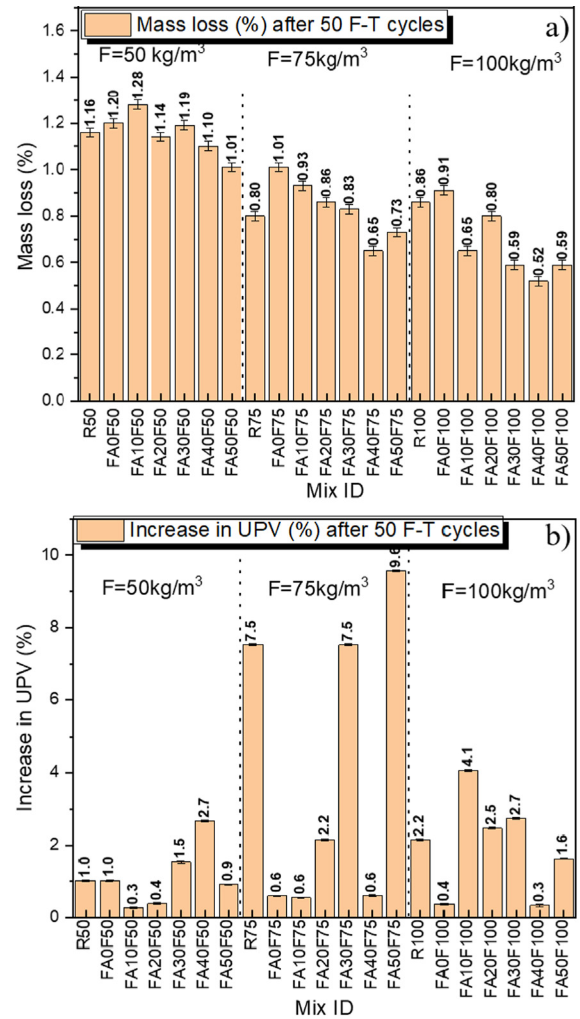

Fig. 14. a) Mass loss and b) Change in UPV results of foam concretes after 50F-T cycles.

the highest mass loss and FA40F100 had the lowest mass loss. Fig. 14b plots the results of UPV variations after 50F-T cycles. As plotted in Fig. 14b, all concretes showed enhancements in UPV values after 50F-T cycles. UPV increase varied between 0.3 and 9.8%. FA40F50 with foam content of 50 kg/m^{3}exhibited the highest UPV increase and FA10F50 had the lowest UPV increase. FA10F75, FA40F75 and FA0F75 with foam content of 75 kg/m^3-showed the highest UPV increase and FA10F50 had the lowest UPV increase. FA10F100 with foam content of 100 kg/m^{3}exhibited the highest UPV increase and FA40F100 had the lowest UPV increase.

3.10. $MgSO_4$ and Na_2SO_4 durability assessment

Foam concretes were placed in 5% $MgSO_4$ and 5% Na_2SO_4 solutions after 91 days of curing. Before the foam concretes are put into sulphate solutions, their initial weights are recorded. Weight loss and compressive strength of foam concretes kept in sulphate solutions for 150 days were determined. Sulphate solutions were renewed every week (1 in 7 days) in the 1st month. The solution was renewed after 15 days in next month. As of the 3rd month, the solution was changed once a month.

3.10.1. Compressive and flexural strength after $MgSO_4$ exposure

Fig. 15a plots the compressive strength of 91-aged concretes and 150-aged sulfate-exposed foam concrete mixtures. As shown in Fig. 15a, all-foam concrete mixtures showed compressive strength reduction after sulphate exposure and strength reductions generally increased with increasing foam content. This strength decrease is because of the conversion of hydration products into non-binding products like ettringite, gypsum, brucite and thaumasite [87]. The positive influence of HFs on concrete strengths exposed to sulphate solutions were more obvious at 75 and 100 kg/m^3 F. 50% FA blended concrete with foam of 50 kg/m^3 exhibited the lowest strength reduction of 4.7% and the highest reduction of 23% was obtained for the mixture containing 30% FA. 10% FA blended concrete with foam of 75 kg/m^{3}revealed the lowest strength reduction of 4.8% and the highest reduction of 64.5% was obtained for the mixture containing 30% FA. 10% FA blended concrete with foam of 100 kg/m^{3}exhibited the lowest strength reduction of 11.2% and the highest reduction of 63.9% was obtained for the reference mixture R100.

Fig. 15b plots the flexural strength of 91-aged foam concrete mixtures and 150-aged sulfate-exposed concretes. As seen in Fig. 15b, all foam concrete mixtures showed flexural strength reduction after sulphate exposure and strength reductions generally increased with rising foam volume. The positive influence of

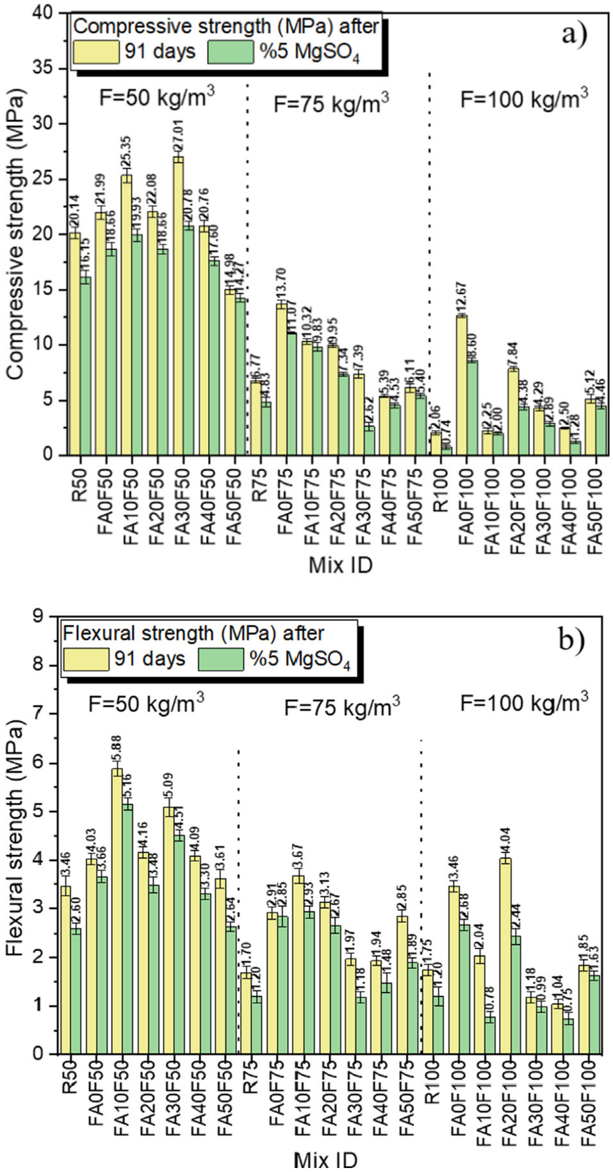

Fig. 15. a) Compressive strengths and b) Flexural strengths of foam concretes at 91 days and after 5% $MgSO_4$ exposure.

HFs on flexural strength of concretes exposed to sulphate solutions were more obvious at 50 and 75 kg/m^3 F. 0% FA blended concrete with foam of 50 kg/m^{3}containing 0.75% HFs exhibited the lowest strength reduction of 9% and the highest reduction of 27.1% was obtained for the mixture containing 50% FA. 0% FA blended concrete with foam of 75 kg/m^{3}containing 1.5% HFs revealed the lowest strength reduction of 2.1% and the highest reduction of 40.15% was obtained for the mixture containing 30% FA. 50% FA blended concrete with foam of 100 kg/m^{3}exhibited the lowest strength reduction of 11.4% and the highest reduction of 61.6% was obtained for the mixture with 10% FA.

3.10.2. Compressive and flexural strength after Na_2SO_4 exposure

Fig. 16a plots the compressive strength of 91-aged concretes and 150-aged Na_2SO_4-exposed foam concrete mixtures. As shown in Fig. 16a, all foam concrete mixtures showed compressive strength reduction after sulphate exposure and strength reductions generally increased with increasing foam content. This strength decline is because of conversion of hydration products into non-binding products like ettringite, gypsum, brucite and thaumasite [87]. The positive influence of HFs on concrete strength exposed to sulphate solutions were more obvious at all foam contents because when compared the reference concretes, HFs added foam concretes had lower strength reduction. Similar to $MgSO_4$ exposed concretes, 50% FA blended concrete having 50 kg/m^3 F exhibited the lowest strength reduction of 1.1% and the highest reduction of 19.7% was obtained for the mixture containing 30% FA. 40% FA blended concrete with foam volume of 75 kg/m^3 revealed the lowest strength reduction of 3% and the highest reduction of 79.3% was obtained for the mixture containing 30% FA. 10% and 40% FA blended concrete with foam content of 100 kg/m^{3}exhibited strength enhancement of 26% and 17.7% respectively and the highest reduction of 48.3% was obtained for the reference mixture R100.

Fig. 16b plots the flexural strength of 91-aged foam mixtures and 150-aged sulfate-exposed foam concrete mixtures. As seen in Fig. 16b, all foam concrete mixtures showed flexural strength reduction after sulphate exposure and strength reductions generally increased with rising foam volume. Positive influence of HFs

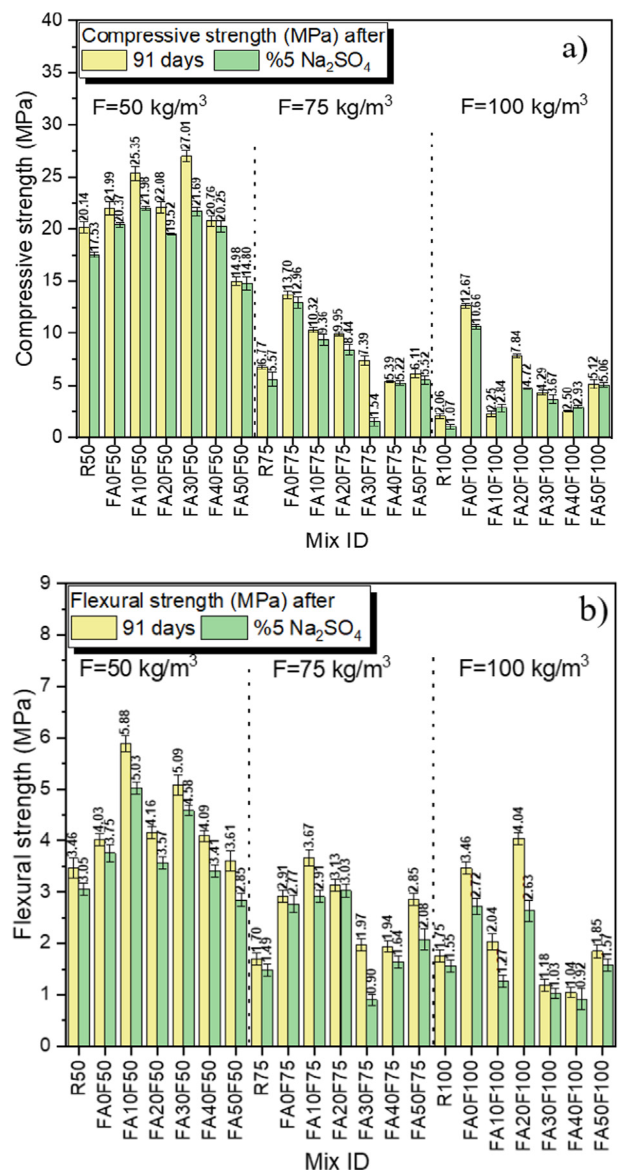

Fig. 16. a) Compressive strengths and b) Flexural strengths of foam concretes at 91 days and after 5% Na_2SO_4 exposure.

on flexural strength of concretes exposed to sulphate solutions were more obvious at 50 and 75 kg/m^3 F. Similar to $MgSO_4$ exposed concretes, 0% FA blended concrete having 50 kg/m^3 F containing 0.75% HFs exhibited the lowest strength reduction of 6.7% and the highest reduction of 21.3% was obtained for the mixture containing 50% FA. 20% FA blended concrete foam content of 75 kg/m^3-containing 1.5% HFs revealed the lowest strength reduction of 3.5% and the highest reduction of 54.3% was obtained for the mixture containing 30% FA. Reference concrete having 100 kg/m^3 F exhibited the lowest strength reduction of 11.4% and the highest reduction of 37.4% was obtained for the mixture with 10% FA.

3.10.3. Mass loss results of foam concretes after MgSO4 and Na_2SO_4 exposure

Fig. 17a shows the mass loss of 150-aged sulfate-exposed foam concrete mixtures. As plotted in Fig. 17a, all mixtures showed very similar mass loss values. A slight enhancement in mass loss were observed with increasing foam content. 30% FA blended concrete with foam content of 50 kg/m^{3}exhibited the lowest mass loss and the mixture containing 50% FA exhibited the highest mass loss of 3.66%. 0% FA blended with foam content of 75 kg/m^{3}concrete

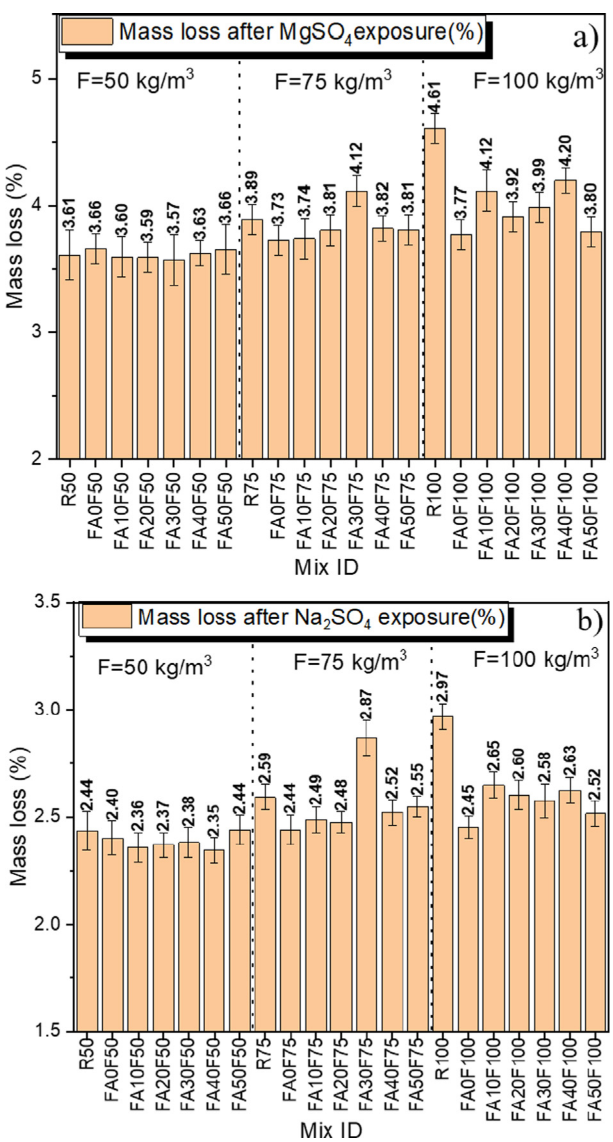

Fig. 17. Mass loss of concretes a) after 5% $MgSO_4$ exposure b) after 5% Na_2SO_4 exposure.

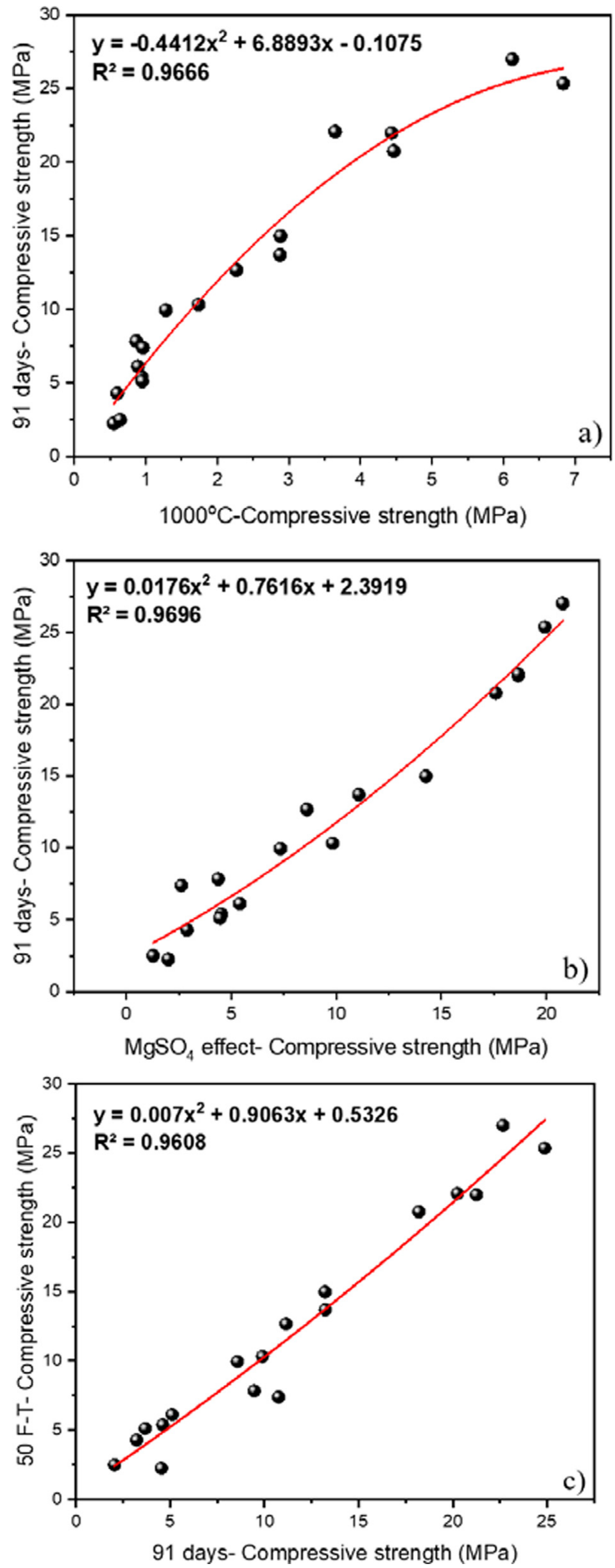

Fig. 18. Correlation among compressive strength and durability tests.

revealed the lowest mass loss and the mixture containing 30% FA exhibited the highest mass loss. Reference concrete having 100 kg/m^3 F presented the highest loss and the lowest loss was obtained for the mixture with 0% FA.

Fig. 17b plots the loss of concretes immersed in Na_2SO_4 solution. As plotted in Fig. 17, mass loss generally increased as foam

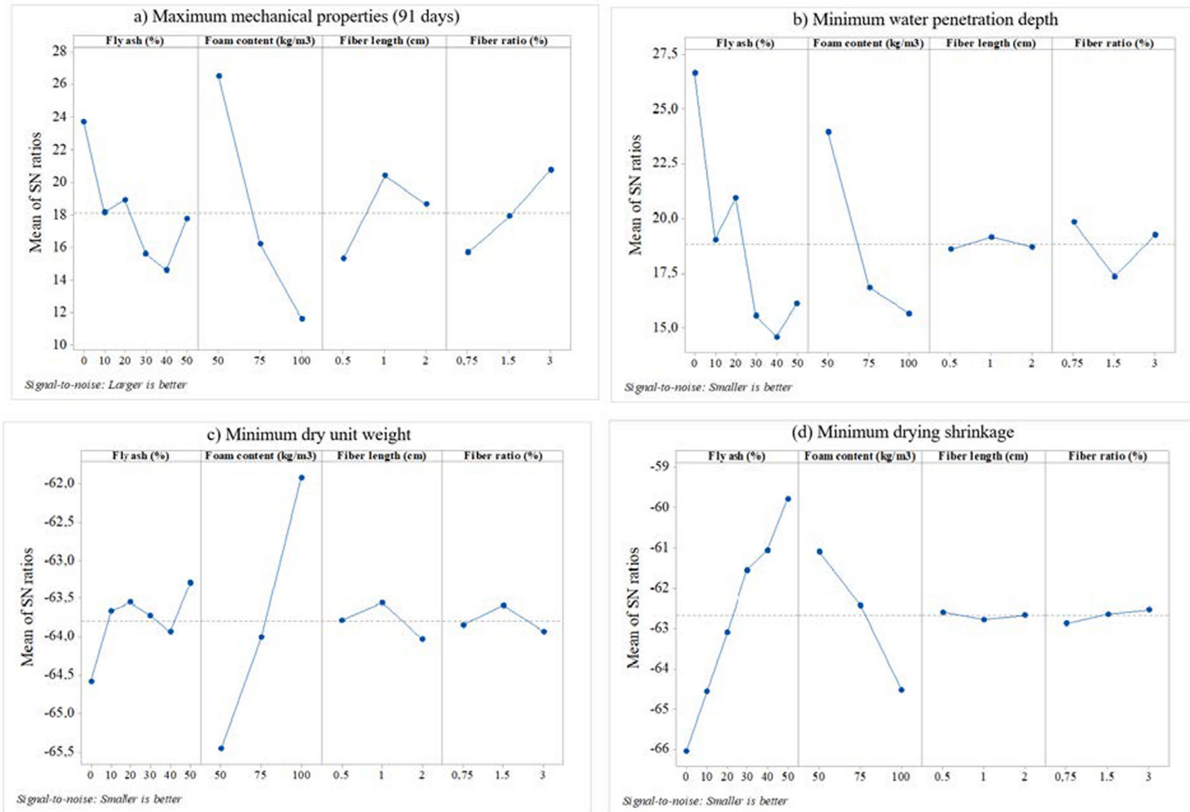

Fig. 19. Relationship between compressive strength and durability tests.

Table 5
Objective function and optimum mixing ratios.

Mixes	Mix ratios				Function
	Fly ash (%)	Foam content (kg/m^3)	Hemp Fiber Ratio (%)	Hemp Fiber Length (cm)	
Optimum mix 1	0	50	3	1	Max. (Mechanical properties)
Optimum mix 2	0	50	0.75	1	Min. (Water penet. Depth)
Optimum mix 3	50	100	1.5	1	Min. (Dry bulk density)
Optimum mix 4	50	50	3	0.5	Min. (Drying shrinkage)

Table 6
Predicted and experimental results for maximum mechanical properties.

Mixes	Compressive strength (MPa)						Flexural strength (MPa)					
	7 Days		28 Days		91 Days		7 Days		28 Days		91 Days	
	Predicted	Experimental	Predicted	Experimental	Predicted	Experimental	Predicted	Experimental	Predicted	Experimental	Predicted	Experimental
Optimum mix 1	19.43	21.11	23.43	25.66	30.21	32.11	3.32	3.25	3.45	3.38	4.22	4.31
Optimum mix 2	16.87	18.87	21.32	23.61	26.53	28.57	3.11	3.02	3.32	3.26	3.72	3.86
Optimum mix 3	1.04	0.89	1.94	1.56	3.62	3.26	0.17	0.21	0.42	0.37	0.51	0.44
Optimum mix 4	6.73	7.65	14.32	12.56	17.63	18.93	1.05	1.11	1.16	1.23	1.39	1.46

Table 7
Predicted and experimental results for drying shrinkage, dry unit weight and water penetration depth.

Mixes	Drying shrinkage - µm (10^{-6})		Dry unit weight (kg/m^3)		Water penetration depth (mm)	
	Predicted	Experimental	Predicted	Experimental	Predicted	Experimental
Optimum mix 1	1803	1888	1994	2045	5.67	5.42
Optimum mix 2	1780	1803	1979	2009	2.43	2.58
Optimum mix 3	1272	1309	1088	1060	9.89	10.56
Optimum mix 4	720	745	1746	1712	7.73	7.55

Table 8
Results of ANOVA analysis.

Two-Way ANOVA (α = 0.05)					
Variables		Compressive and Flexural Strength	Water Penetration Depth	Dry unit weight	Drying Shrinkage
Fly ash (%)	A	0.08	0.28	0.43	0.01
	F value	4.03	1.67	1.15	43.32
	Effect (%)	21.7	23.2	3.0	47.4
	Level of significance	No	No	No	Yes
Foam Content (kg/m^3)	A	0.01	0.04	0.01	0.01
	F value	12.24	5.12	36.99	46.60
	Effect (%)	65.7	71.2	95.0	51.0
	Level of significance	Yes	Yes	Yes	Yes
Fiber length (cm)	A	0.34	0.94	0.64	0.37
	F value	1.32	0.07	0.47	1.18
	Effect (%)	7.1	1.0	1.2	1.3
	Level of significance	No	No	No	No
Fiber Ratio (%)	A	0.48	0.73	0.73	0.75
	F value	1.03	0.33	0.34	0.30
	Effect (%)	5.5	4.6	0.8	0.3
	Level of significance	No	No	No	No

Table 9
Mechanical characteristics of optimization groups after high temperature effect.

Mix ID	250 °C		500 °C		750 °C		1000 °C	
	Flexural Strength	Compressive strength	Flexural Strength	Compressive strength	Flexural Strength	Compressive strength	Flexural Strength	Compressive strength
Optimum mix 1	5.52	35.68	4.48	30.11	2.86	14.32	1.42	7.24
Optimum mix 2	4.48	36.26	4.01	28.87	2.41	11.78	1.16	6.89
Optimum mix 3	0.89	1.90	0.61	1.76	0.32	1.09	0	0.57
Optimum mix 4	2.04	23.41	1.86	21.63	1.54	10.88	0.85	5.89

content increased due to increasing porosity. 40% FA blended concrete with foam content of 50 kg/m^{3}exhibited the lowest mass loss and the mixtures containing 50% FA and R50 exhibited the highest mass loss. 0% FA blended concrete with foam content of 75 kg/m^3-exhibited the lowest loss and the highest loss was observed for mixture having 30% FA. Reference having 100 kg/m^3 F presented the highest loss and the lowest loss was obtained for the mixture with 0% FA.

3.11. Taguchi optimization

Four different optimizations were carried out for foam concretes belonging to the Taguchi L18 matrix. In the first group values after 91 days of compressive and flexural strengths were optimized according to maximized function. The water penetration depth determined by the 2nd group capillary test was optimized according to the minimized function. The 3rd group has been optimized with a minimized function to improve thermal properties and reduce dead loads. Group 4 has been optimized with minimized function to reduce 120-day drying shrinkage. Since high R^2 values were obtained between the compressive strengths obtained after MgSO4. Freeze-thaw and high temperature effects and 91-day compressive strengths. Only mechanical properties were used in optimization. As the compressive strength of foam concrete increases. Its resistance against physical and chemical effects also increases. The correlation between the compressive strengths for 91 days and compressive strength obtained by means of durability tests is given in Fig. 18.

S/N ratios of optimization groups are presented in Fig. 19. For maximum compressive and flexural strength. FA content should be 0% and the foam content should be 50 kg/m^3. A fiber length of 1 cm and a ratio of 3% improves the mechanical properties (Fig. 19a). In Fig. 19b, FA ratio should be 0% and the foam content should be 50 kg/m^3 for the minimum water processing depth. No significant influence of fibre length on water penetration depth was observed. Fiber ratio was determined as 0.75% for the minimum depth of water penetration. In Fig. 19c, for the minimum dry unit weight. FA should be 50% and the foam content should be 100 kg/m^3. Dry unit weight values decrease when fiber length and ratio are 1 cm and 1.5% respectively. In Fig. 19d, a significant effect of the fiber on drying shrinkage was not observed. If FA is 50% and F is 50 kg/m^3. The drying shrinkage values decrease.

Table 5 presents optimum mixing ratios for maximum and minimum functions according to S/N ratios.

Validation experiments were carried out for the mixing ratios determined as a result of the optimization. Prediction and experimental results for the maximum mechanical properties for the 1st group are illustrated in Table 6. In Table 6, 91-day compressive strength of the optimum mix1 mixture developed for maximum mechanical properties was estimated as 30.21 MPa. The verification test & measured 32.11 MPa with a difference of 6.3.

Table 7 shows the prediction and experimental results of the optimum mixture recommended for the minimum water penetration depth. The optimum mix2 developed for the 28th day of the water penetration depth was determined as 2.58 mm with a 6.2% difference. Water penetration depths of the mixtures vary between 2.58 and 10.56. Table 7 also shows the prediction and experimental results of the optimization for the minimum dry unit weight. The weight of optimum mix3 has been measured as 1060 kg/m^3. The optimum mix3 reduced the dry unit weight by 48.2% compared to the optimum mix1 mixture. In Table 7, the estimation and experimental results of the optimum mixture developed for mini-

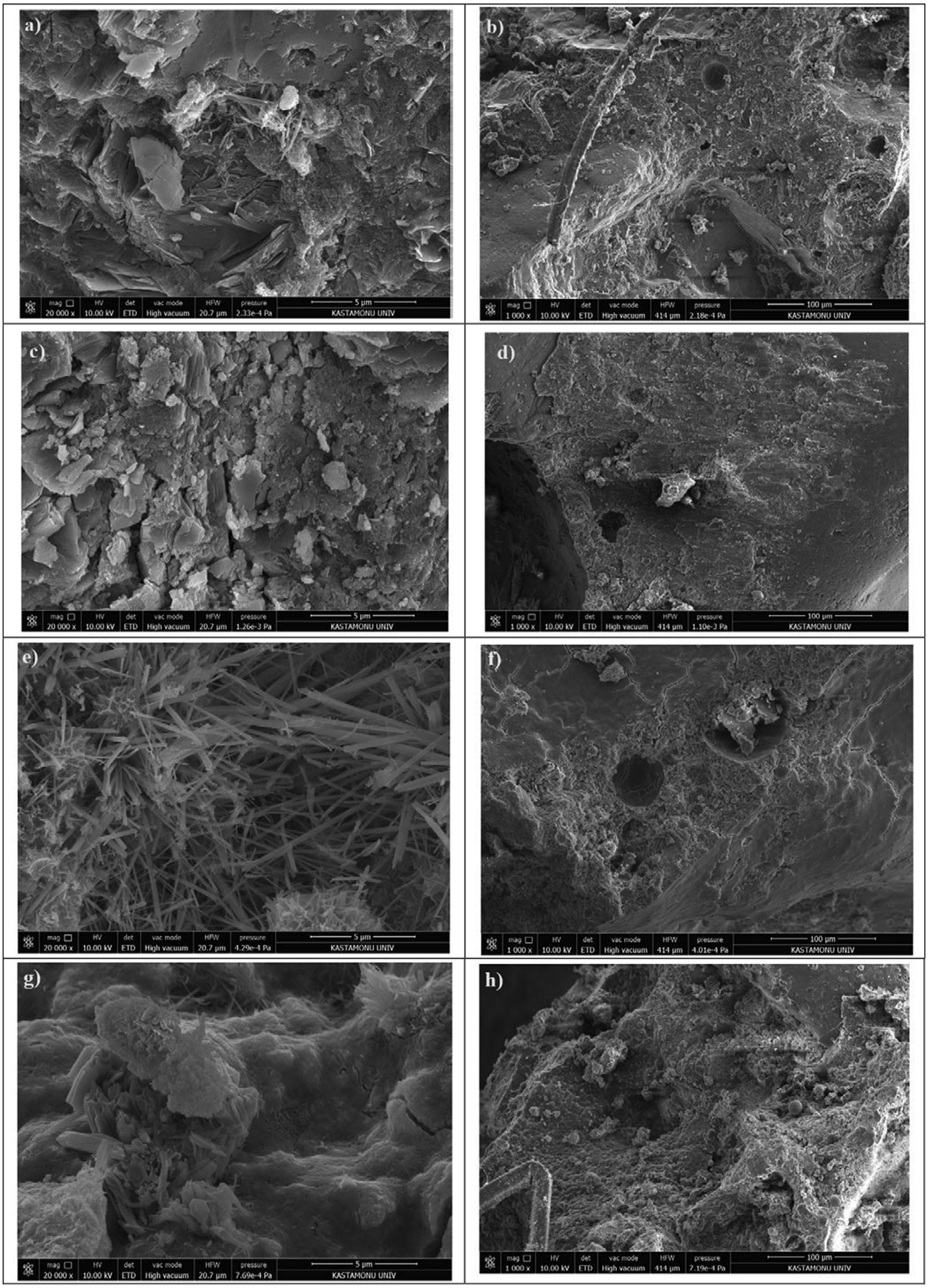

Fig. 20. SEM views of optimum mix1 (a.b); optimum mix2 (c.d); optimum mix3 (e.f) and optimum mix4 (g.h) concretes.

mum drying shrinkage are presented. The drying shrinkage value of the optimum mix4 mixture was measured as 745×10^{-6} on the 120th day. With the optimization carried out, the drying shrinkage value was reduced below 800×10^{-6}.

It is seen that optimization models applied for 4 different purposes are quite successful. In the optimum mix1 mixture with a dry unit weight value of approximately 2000 kg/m^3, a compressive strength above 30 MPa was obtained on the 91st day. These results show that foam concretes can also be used in structural designs. In addition, dry unit weight values have been reduced to approximately 1000 kg/m^3 with the optimization made. ANOVA analyzes of the purpose functions used for optimization are presented in Table 8. The only variation in foam rate was significant in respect to compressive and flexural strengths. Change in FA rate on compressive and flexural strengths is 21.7%. Change in foam content is effective by 65.7%. In terms of the depth of water treatment, the effect rate was determined to be 71.2%, while only the change in foam content was significant. The change in fly ash content has an effect of 23.2% on the depth of water treatment. Similar results are observed in dry unit weight values. A statistical significance was observed for the change in fly ash and foam content in drying shrinkage. The change in fly ash and foam content can be effective in drying shrinkage by 47.4% and 51%, respectively. Positive or negative influence of the fiber properties for physical and mechanical characteristics of foam concretes has not been observed. Change of FA and foam content in foam concrete design is more effective and meaningful. The use of FA in foam concretes, CO_2 emissions and environmental impacts will be reduced.

For the optimization groups, the high temperature effect was also investigated from the durability experiments. Experimental results of flexural and compressive strengths at different temperatures are seen in Table 9.

3.12. SEM analysis

SEM (Scanning electron microscope) images of concretes after room and high temperature were plotted in Figs. 20 and 21. At lower magnifications, the samples exhibit a compact

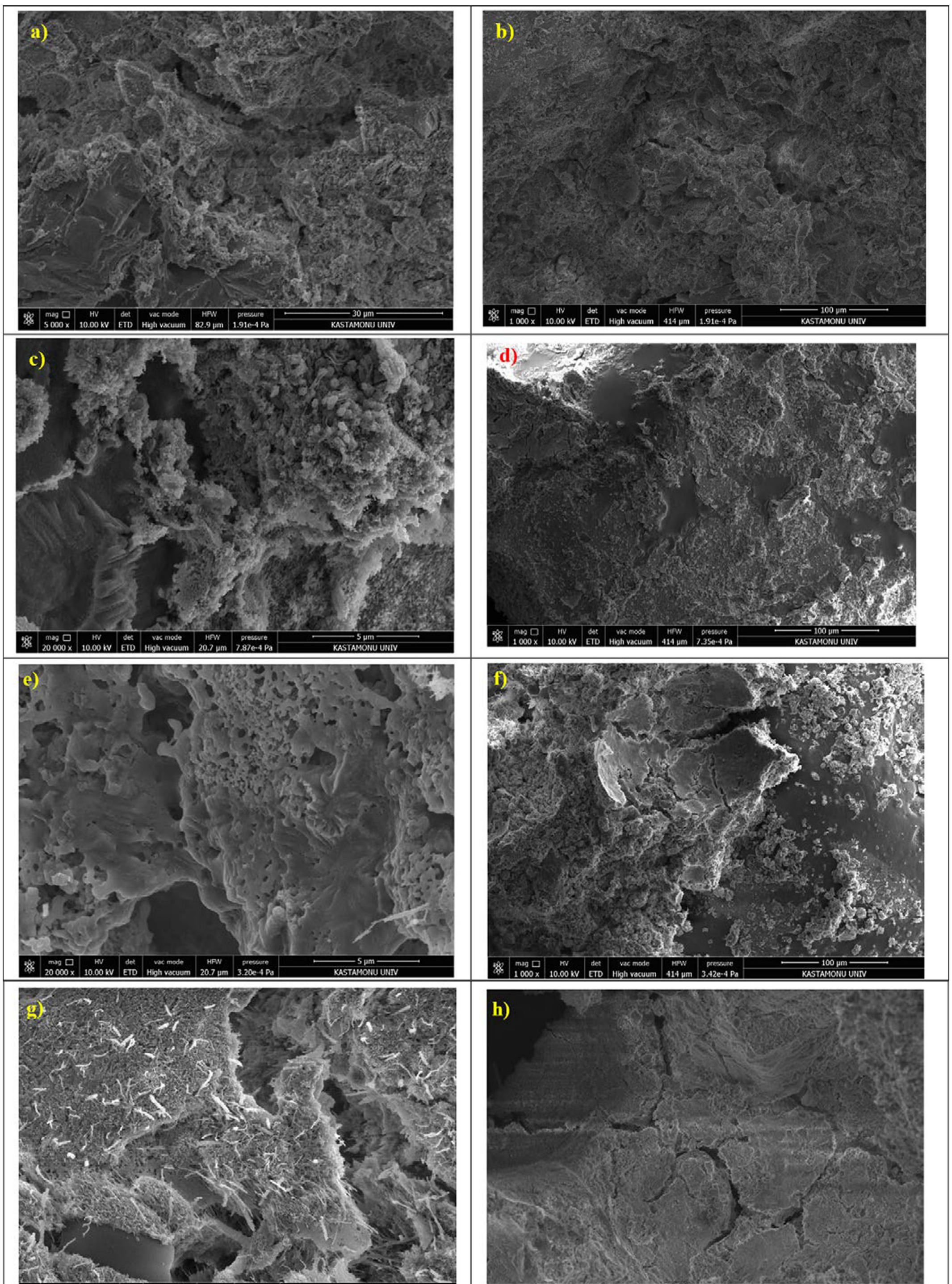

Fig. 21. SEM views of optimum mix1 (a.b); optimum mix2 (c.d); optimum mix3 (e.f) and optimum mix4 (g.h) concretes behind 1000 °C.

microstructure containing pores up to 100 μm. Fig. 20a shows CSH crystals and CH plates in microstructure images of optimum mix 1. In Fig. 20b, hemp fiber and air bubbles are seen in the microstructure images of optimum mix 1. CH plates and micro-cracks are seen in the microstructure images of Optimum mix 2 (Fig. 20c-d). Micro-cracks were formed due to the high drying shrinkage behavior of foam concrete. Intense CH presence was observed as FA was not used in Optimum mix 1 and 2. It was determined that secondary CSH gels were formed by consuming CH due to pozzolanic reactions in FA mixtures. It has also been observed that large CH plates fill the gaps between cement and fine aggregate particles. In Fig. 20e, dense CSH gels were observed in the microstructure view of optimum blend 3 with 50% fly ash. The use of high amounts of binders (FA + cement) in foam concretes manufactured CSH makes the gels denser. This has also contributed to the formation of dense structures in secondary CSH formation using FA. Fig. 20f shows air bubbles in the microstructure and micro-cracks in the air bubbles. In Fig. 20g-h, CSH gels, CH plates, and hemp fibers were observed in SEM views of optimum mix 3.

Fig. 21 determined that the high-temperature effect damaged CSH gels in optimum mixtures. All hydration products, possessing CSH and CH, have emerged as amorphous forms that have lost their crystal structures due to the high temperature effect. Small round structures were observed instead of CSH crystals after exposure to high temperature (Fig. 21e). It was observed that generally, cracks are made in the microstructure after a time at high temperatures. It was determined that by means of breakdown of hydration products, a micro-crack network was formed. It was also observed that aggregates were separated from the matrix by means of high-temperature impact. The micro crack network formed is one of the reasons for the loss of strength in foam concretes. Microcracks were caused by the dehydration of cement paste due to high temperature effect and morphological changes in ITZ. It was determined that hemp fibers were melted with the effect of 1000 °C in SEM pictures. The melting of these fibers at high temperatures will also help reduce the vapor pressure that will occur in the concrete.

4. Conclusions

Investigation on mechanical, microstructural, durability and thermal characteristics of hemp fibers (HFs) reinforced foam concretes with fly ash (FA) and Taguchi optimization approach were performed and the following conclusions have been noted:

- With increasing F content, the mixtures revealed higher slump values due to decreasing solid content. Replacing fly ash with ordinary Portland cement enhanced the slump flow diameter because of the small round-shape and smooth surface of the FA's grains and but inclusion of HFs had a negative impact on the slump values due to the increase in water absorption amount with HFs content.
- The addition of HFs results in high compressive strength enhancements at high foam contents and high later-age compressive strength was observed for mixture having 30% FA at low foam contents.
- Joint usage of 10% FA and HFs presented the highest flexural strength at 50 and 75 kg/m^3 F and joint usage of 20% FA and HFs presented the highest flexural strength at 100 kg/m^3 F.
- Dry unit weight and thermal conductivity declined by increment of foam volume and the lowest rates were obtained for mixtures containing 50%, 40% and 30% FA at foam contents of 50, 75 and 100 kg/m^3 F respectively.
- Drying shrinkage of foam concretes raised by increment of foam volume but declined by increment of FA content. HFs affected the drying shrinkage positively more especially at low foam content and it seems HFs reduced drying shrinkage slightly at high foam contents.
- The sorptivity of foam concretes increased with increasing foam content due to decreasing solid content and increasing porosity. The sorptivity of foam concretes increased with increasing foam content due to decreasing solid content and increasing porosity.
- FA10F75 with 3% HFs exhibited the lowest sorptivity with sorptivity reduction of 23.15% compared to R75 and FA50F75 with 3% HFs had also lower sorptivity than FA40F75 which had the highest sorptivity with an increase of 41.78% compared to R75.
- FA50F100 also showed lower sorptivity with a decrease of 16.15% than R100. FA30F100 and FA40F100 with 1.5% HFs content had very higher sorptivity than R100 and FA30F100 depicted the highest sorptivity with an increase of 61.81% compared to R100.
- The compressive strength of all concretes performed very well and generally enhanced after temperature exposure of 250 °C and 500 °C in comparison with the compressive strength at 20 °C.
- The concretes containing 40% FA with foam content of 75 and 100 kg/m^3 performed best compressive strength resistance to all high temperature ranges.
- It can be noted that the mixture with HFs had higher strength increase than R50 but after 750 °C, the strength reduction of these two mixtures were nearly the same. FA10F50 and FA50F50 performed the best temperature performance at 500 °C and FA10F50 gained the highest strength at 500 °C when compared to strength at ambient temperature. At 750 °C, FA40F50 and FA50F50 exhibited the best performance with the strength reduction of 32 and 37.6% when compared to strength at ambient temperature respectively.
- At 500 °C and 750 °C, FA30F50 revealed the best high temperature flexural strength performance with an enhancement of 0.24% and a reduction of 65% respectively. At 500 °C and 750 °C, FA0F100 showed the best temperature resistance with an increase of 12.6% and a reduction of 68.2% respectively,
- 30% FA blended foam concrete performed the best at F-T exposure at 75 kg/m^3 F. At 100 kg/m^3 F, very huge strength enhancement as 309% was observed for the reference concrete R100. In this foam content, 10%FA blended concrete showed the best performance with strength increase of 106.4% and the strength enhancement decreased with increasing after 10% FA content.
- The positive influence of HFs on compressive strength of concretes exposed to sulphate solutions were more obvious at 75 and 100 kg/m^3 F. 50% FA blended concrete with 50 kg/m^3 F exhibited the lowest strength reduction as 4.7% and the highest reduction as 23% was obtained for the mixture containing 30% FA.

CRediT authorship contribution statement

Osman Gencel: Conceptualization, Methodology, Writing - review & editing. **Oguzhan Yavuz Bayraktar:** Writing - original draft. **Gokhan Kaplan:** Writing - original draft. **Ahmet Benli:** Methodology, Writing - original draft. **Gonzalo Martínez-Barrera:** Data curation, Writing - review & editing. **Witold Brostow:** Data curation, Writing - review & editing. **Murat Tek:** Investigation, Resources. **Burak Bodur:** Investigation, Resources.

Declaration of Competing Interest

The authors declare that they have no known competing financial interests or personal relationships that could have appeared to influence the work reported in this paper.

References

[1] F. Koksal, Y. Sahin, O. Gencel, Influence of expanded vermiculite powder and silica fume on properties of foam concretes, Constr. Build. Mater. 257 (2020) 1–16.
[2] O.H. Oren, A. Gholampour, O. Gencel, T. Ozbakkaloglu, Physical and mechanical properties of foam concretes containing granulated blast furnace slag as fine aggregate, Constr. Build. Mater. 238 (2020) 1–9.
[3] M. Kozłowski, M. Kadela, Mechanical Characterization of Lightweight Foamed Concrete, Adv. Mater. Sci. Eng. 2018 (2018) 1–8.
[4] M.A.O. Mydin, Y.C. Wang, Mechanical properties of foamed concrete exposed to high temperatures, Constr. Build. Mater. 26 (1) (2012) 638–654.
[5] J.J.D. Diaz, F.P. Alvarez-Rabanal, O. Gencel, P.J.G. Nieto, M. Alonso-Martinez, A. Navarro-Manso, B. Prendes-Gero, Hygrothermal study of lightweight concrete hollow bricks: A new proposed experimental-numerical method, Energy Build. 70 (2014) 194–206.
[6] B. Raj, D. Sathyan, M.K. Madhavan, A. Raj, Mechanical and durability properties of hybrid fiber reinforced foam concrete, Constr. Build. Mater. 245 (2020).
[7] P.O. Awoyera, B.F. Britto, Foamed concrete incorporating mineral admixtures and pulverized ceramics: Effect of phase change and mineralogy on strength characteristics, Constr. Build. Mater. 234 (2020).
[8] D. Falliano, D. De Domenico, G. Ricciardi, E. Gugliandolo, Compressive and flexural strength of fiber-reinforced foamed concrete: Effect of fiber content, curing conditions and dry density, Constr. Build. Mater. 198 (2019) 479–493.
[9] C. Sun, Y. Zhu, J. Guo, Y.M. Zhang, G.X. Sun, Effects of foaming agent type on the workability, drying shrinkage, frost resistance and pore distribution of foamed concrete, Constr. Build. Mater. 186 (2018) 833–839.
[10] M. Drusa, L. Fedorowicz, M. Kadela, W. Scherfel, Application of geotechnical models in the description of composite foamed concrete used in contact layer with the subsoil, Proceedings of the 10th Slovak Geotechnical Conference "Geotechnical problems of engineering constructions, 2011.
[11] L. Fedorowicz, M. Kadela, Ł. Bednarski, Modeling of the foamed concrete behavior for the layered structures cooperating with subsoil, Technical Notes of Katowice School of Technology 6 (2014) 73–81.
[12] M. Kadela, M. Kozłowski, Foamed concrete layer as sub-structure of industrial concrete floor, Procedia Eng. 161 (2016) 468–476.
[13] I. Tekin, M.Y. Durgun, O. Gencel, T. Bilir, W. Brostow, H.E.H. Lobland, Concretes with synthetic aggregates for sustainability, Constr. Build. Mater. 133 (2017) 425–432.
[14] W. She, Y. Du, G.T. Zhao, P. Feng, Y.S. Zhang, X.Y. Cao, Influence of coarse fly ash on the performance of foam concrete and its application in high-speed railway roadbeds, Constr. Build. Mater. 170 (2018) 153–166.
[15] T. Bilir, O. Gencel, I.B. Topcu, Properties of mortars with fly ash as fine aggregate, Constr. Build. Mater. 93 (2015) 782–789.
[16] A. Khodabakhshian, J. de Brito, M. Ghalehnovi, E.A. Shamsabadi, Mechanical, environmental and economic performance of structural concrete containing silica fume and marble industry waste powder, Constr. Build. Mater. 169 (2018) 237–251.
[17] Z. Prosek, V. Nezerka, P. Tesarek, Enhancing cementitious pastes with waste marble sludge, Constr. Build. Mater. 255 (2020).
[18] B. Demirel, The effects of waste marble dust applying as a fine sand on the mechanical properties of concrete, Cem Wapno Beton 15 (5) (2010) 259-+.
[19] K.K. Das, E.S.S. Lam, H.H. Tang, Partial replacement of cement by ground granulated blast furnace slag and silica fume in two-stage concrete (preplaced aggregate concrete), Structural Concrete (2020).
[20] Q. Li, Z. Li, G. Yuan, Effects of elevated temperatures on properties of concrete containing ground granulated blast furnace slag as cementitious material, Constr. Build. Mater. 35 (2012) 687–692.
[21] Y. Zhang, D. Chen, Y. Liang, K. Qu, K. Lu, S. Chen, M. Kong, Study on engineering properties of foam concrete containing waste seashell, Constr. Build. Mater. 260 (2020).
[22] O. Gencel, Effect of elevated temperatures on mechanical properties of high-strength concrete containing varying proportions of hematite, Fire Mater. 36 (3) (2012) 217–230.
[23] O. Gencel, W. Brostow, T. Datashvili, M. Thedford, Workability and Mechanical Performance of Steel Fiber-Reinforced Self-Compacting Concrete with Fly Ash, Compos. Interfaces 18 (2) (2011) 169–184.
[24] J.F. Castillo-Lara, E.A. Flores-Johnson, A. Valadez-Gonzalez, P.J. Herrera-Franco, J.G. Carrillo, P.I. Gonzalez-Chi, Q.M. Li, Mechanical Properties of Natural Fiber Reinforced Foamed Concrete, Materials 13 (14) (2020).
[25] F. Sarasini, J. Tirillo, C. Sergi, M.C. Seghini, L. Cozzarini, N. Graupner, Effect of basalt fibre hybridisation and sizing removal on mechanical and thermal properties of hemp fibre reinforced HDPE composites, Compos. Struct. 188 (2018) 394–406.
[26] I.N. Grubega, B. Markovic, A. Gojevic, J. Brdaric, Effect of hemp fibers on fire resistance of concrete, Constr. Build. Mater. 184 (2018) 473–484.
[27] N. Mostefai, R. Hamzaoui, S. Guessasma, A. Aw, H. Nouri, Microstructure and mechanical performance of modified hemp fibre and shiv mortars: Discovering the optimal formulation, Mater. Des. 84 (2015) 359–371.
[28] B. Çomak, A. Bideci, Ö. Salli Bideci, Effects of hemp fibers on characteristics of cement based mortar, Constr. Build. Mater. 169 (2018) 794–799.
[29] R. Hamzaoui, S. Guessasma, K. Abahri, O. Bouchenafa, Formulation of Modified Cement Mortars Using Optimal Combination of Fly Ashes, Shiv, and Hemp Fibers, J. Mater. Civ. Eng. 32 (2) (2020).
[30] G. Ruano, F. Bellomo, G. López, A. Bertuzzi, L. Nallim, S. Oller, Mechanical behaviour of cementitious composites reinforced with bagasse and hemp fibers, Constr. Build. Mater. 240 (2020).
[31] R. Hamzaoui, S. Guessasma, B. Mecheri, A.M. Eshtiaghi, A. Bennabi, Microstructure and mechanical performance of modified mortar using hemp fibres and carbon nanotubes, Mater. Des. 56 (2014) 60–68.
[32] O. Gencel, M. Oguz, A. Gholampour, T. Ozbakkaloglu, Recycling waste concretes as fine aggregate and fly ash as binder in production of thermal insulating foam concretes, Journal of Building, Engineering (2021).
[33] E.P. Kearsley, P.J. Wainwright, The effect of high fly ash content on the compressive strength of foamed concrete, Cem. Concr. Res. 31 (1) (2001) 105–112.
[34] H.S. Gokce, D. Hatungimana, K. Ramyar, Effect of fly ash and silica fume on hardened properties of foam concrete, Constr. Build. Mater. 194 (2019) 1–11.
[35] R. Gopalakrishnan, V.M. Sounthararajan, A. Mohan, M. Tholkapiyan, The strength and durability of fly ash and quarry dust light weight foam concrete, Mater Today-Proc 22 (2020) 1117–1124.
[36] A. Benli, Mechanical and durability properties of self-compacting mortars containing binary and ternary mixes of fly ash and silica fume, Structural Concrete 20 (3) (2019) 1096–1108.
[37] A. Benli, M. Karatas, E. Gurses, Effect of sea water and MgSO4 solution on the mechanical properties and durability of self-compacting mortars with fly ash/silica fume, Constr. Build. Mater. 146 (2017) 464–474.
[38] A. Benli, M. Karatas, Y. Bakir, An experimental study of different curing regimes on the mechanical properties and sorptivity of self-compacting mortars with fly ash and silica fume, Constr. Build. Mater. 144 (2017) 552–562.
[39] O.H. Oren, A. Gholampour, O. Gencel, T. Ozbakkaloglu, Physical and mechanical properties of foam concretes containing granulated blast furnace slag as fine aggregate, Constr. Build. Mater. 238 (2020).
[40] F. Koksal, Y. Sahin, O. Gencel, Influence of expanded vermiculite powder and silica fume on properties of foam concretes, Constr. Build. Mater. 257 (2020).
[41] F. Kesikidou, M. Stefanidou, Natural fiber-reinforced mortars, Journal of Building Engineering 25 (2019).
[42] X.L. Xie, Z.W. Zhou, M. Jiang, X.L. Xu, Z.Y. Wang, D. Hui, Cellulosic fibers from rice straw and bamboo used as reinforcement of cement-based composites for remarkably improving mechanical properties, Compos Part B-Eng 78 (2015) 153–161.
[43] M. Khorami, E. Ganjian, Comparing flexural behaviour of fibre-cement composites reinforced bagasse: Wheat and eucalyptus, Constr. Build. Mater. 25 (9) (2011) 3661–3667.
[44] N.G. Ozerkan, B. Ahsan, S. Mansour, S.R. Iyengar, Mechanical performance and durability of treated palm fiber reinforced mortars, International Journal of Sustainable Built Environment 2 (2) (2013) 131–142.
[45] N.M. Altwair, M.A.M. Johari, S.F.S. Hashim, Shrinkage Characteristics of Green Engineered Cementitious Composites with Varying Palm Oil Fuel Ash Contents and Water-Binder Ratios, Advanced Materials Engineering and Technology 626 (2012) 245-+.
[46] G. Ramakrishna, T. Sundararajan, Impact strength of a few natural fibre reinforced cement mortar slabs: a comparative study, Cement Concrete Comp 27 (5) (2005) 547–553.
[47] X.M. Zhou, S.H. Ghaffar, W. Dong, O. Oladiran, M.Z. Fan, Fracture and impact properties of short discrete jute fibre-reinforced cementitious composites, Mater. Des. 49 (2013) 35–47.
[48] ASTM, ASTM C1437 - 15 Standard Test Method for Flow of Hydraulic Cement Mortar.West Conshohocken, PA: ASTM International., 2015.
[49] ASTM, C642–13 Standard Test Method for Density, Absorption, and Voids in Hardened Concrete. West Conshohocken, PA: ASTM, International (2013, 2013.).
[50] ASTM, ASTM C348 - 19 Standard Test Method for Flexural Strength of Hydraulic-Cement Mortars. ASTM International, West Conshohocken, PA., 2019.
[51] ASTM, ASTM C349 - 18 Standard Test Method for Compressive Strength of Hydraulic-Cement Mortars (Using Portions of Prisms Broken in Flexure).ASTM International, West Conshohocken, PA., 2018.
[52] ASTM, ASTM C1585 - 20 Standard Test Method for Measurement of Rate of Absorption of Water by Hydraulic-Cement Concretes,West Conshohocken, PA: ASTM International, 2020.
[53] ASTM, D7984–16 Standard Test Method for Measurement of Thermal Effusivity of Fabrics Using a Modified Transient Plane Source (MTPS) Instrumen, ASTM, International (2016).
[54] ASTM, ASTM C596 - 18 Standard Test Method for Drying Shrinkage of Mortar Containing Hydraulic Cement,West Conshohocken, PA: ASTM International., 2018.
[55] ASTM, ASTM C 666-97, Standard Test Method for Resistance of Concrete to Rapid Freezing and Thawing,West Conshohocken, PA: ASTM International., 2015.
[56] ASTM, ASTM C597-02, Standard Test Method for Pulse Velocity through Concrete,West Conshohocken, PA: ASTM International, 2003.
[57] M. Gesoglu, E. Ozbay, Effects of mineral admixtures on fresh and hardened properties of self-compacting concretes: binary, ternary and quaternary systems, Mater. Struct. 40 (9) (2007) 923–937.
[58] X.M. Chen, Y. Yan, Y.Z. Liu, Z.H. Hu, Utilization of circulating fluidized bed fly ash for the preparation of foam concrete, Constr. Build. Mater. 54 (2014) 137–146.

[59] J. Jiang, Z.Y. Lu, Y.H. Niu, J. Li, Y.P. Zhang, Study on the preparation and properties of high-porosity foamed concretes based on ordinary Portland cement, Mater. Des. 92 (2016) 949–959.
[60] Y. Xie, J. Li, Z.Y. Lu, J. Jiang, Y.H. Niu, Effects of bentonite slurry on air-void structure and properties of foamed concrete, Constr. Build. Mater. 179 (2018) 207–219.
[61] M.Y.J. Liu, U.J. Alengaram, M. Santhanam, M.Z. Jumaat, K.H. Mo, Microstructural investigations of palm oil fuel ash and fly ash based binders in lightweight aggregate foamed geopolymer concrete, Constr. Build. Mater. 120 (2016) 112–122.
[62] A. Benli, M. Karatas, H.A. Toprak, Mechanical characteristics of self-compacting mortars with raw and expanded vermiculite as partial cement replacement at elevated temperatures, Constr. Build. Mater. 239 (2020).
[63] D.Y. Yang, M. Liu, Z.M. Ma, Properties of the foam concrete containing waste brick powder derived from construction and demolition waste, Journal of Building Engineering 32 (2020).
[64] S. Cho, J. Kruger, A. van Rooyen, G. van Zijl, Rheology and application of buoyant foam concrete for digital fabrication, Engineering, Composites Part B, 2021, p. 108800.
[65] S.J. Choi, S.S. Lee, P.J.M. Monteiro, Effect of Fly Ash Fineness on Temperature Rise, Setting, and Strength Development of Mortar, J. Mater. Civ. Eng. 24 (5) (2012) 499–505.
[66] M. Seifan, S. Mendoza, A. Berenjian, Mechanical properties and durability performance of fly ash based mortar containing nano- and micro-silica additives, Constr. Build. Mater. 252 (2020).
[67] O. Karahan, C.D. Atis, The durability properties of polypropylene fiber reinforced fly ash concrete, Mater. Des. 32 (2) (2011) 1044–1049.
[68] R. Demirboga, R. Gul, The effects of expanded perlite aggregate, silica fume and fly ash on the thermal conductivity of lightweight concrete, Cem. Concr. Res. 33 (5) (2003) 723–727.
[69] S.N. Shah, K.H. Mo, S.P. Yap, J. Yang, T.-C. Ling, Lightweight foamed concrete as a promising avenue for incorporating waste materials: A review, Resour. Conserv. Recycl. 164 (2021) 105103.
[70] I.K. Harith, Study on polyurethane foamed concrete for use in structural applications, Case Stud. Constr. Mater. 8 (2018) 79–86.
[71] O. Karahan, C.D. Atiş, The durability properties of polypropylene fiber reinforced fly ash concrete, Mater. Des. 32 (2) (2011) 1044–1049.
[72] P. Chindaprasirt, U. Rattanasak, Shrinkage behavior of structural foam lightweight concrete containing glycol compounds and fly ash, Mater. Des. 32 (2) (2011) 723–727.
[73] K. Vardhan, R. Siddique, S. Goyal, Influence of marble waste as partial replacement of fine aggregates on strength and drying shrinkage of concrete, Constr. Build. Mater. 228 (2019).
[74] F.U.A. Shaikh, S.W.M. Supit, Compressive strength and durability properties of high volume fly ash (HVFA) concretes containing ultrafine fly ash (UFFA), Constr. Build. Mater. 82 (2015) 192–205.
[75] A. Kanellopoulos, M.F. Petrou, I. Ioannou, Durability performance of self-compacting concrete, Constr. Build. Mater. 37 (2012) 320–325.
[76] W.Z. Zheng, B.F. Luo, Y. Wang, Microstructure and mechanical properties of RPC containing PP fibres at elevated temperatures, Mag. Concr. Res. 66 (8) (2014) 397–408.
[77] C. Bing, J.Y. Liu, Residual strength of hybrid-fiber-reinforced high-strength concrete after exposure to high temperatures, Cem. Concr. Res. 34 (6) (2004) 1065–1069.
[78] A. Nadeem, S.A. Memon, T.Y. Lo, The performance of Fly ash and Metakaolin concrete at elevated temperatures, Constr. Build. Mater. 62 (2014) 67–76.
[79] S. Ghosh, K.W. Nasser, Effects of high temperature and pressure on strength and elasticity of lignite fly ash and silica fume concrete, Aci Mater J 93 (1) (1996) 51–60.
[80] C.S. Poon, S. Azhar, M. Anson, Y.L. Wong, Comparison of the strength and durability performance of normal- and high-strength pozzolanic concretes at elevated temperatures, Cem. Concr. Res. 31 (9) (2001) 1291–1300.
[81] M.S. Rais, M. Shariq, A. Masood, A. Umar, M.M. Alam, An experimental and analytical investigation into age-dependent strength of fly ash mortar at elevated temperature, Constr. Build. Mater. 222 (2019) 300–311.
[82] Z. Jia, C. Chen, J. Shi, Y. Zhang, Z. Sun, P. Zhang, The microstructural change of C-S-H at elevated temperature in Portland cement/GGBFS blended system, Cem. Concr. Res. 123 (2019).
[83] A. Mendes, J. Sanjayan, F. Collins, Phase transformations and mechanical strength of OPC/Slag pastes submitted to high temperatures, Mater. Struct. 41 (2) (2007) 345–350.
[84] H.Y. Wang, The effects of elevated temperature on cement paste containing GGBFS, Cement Concrete Comp 30 (10) (2008) 992–999.
[85] T. Rahmani, B. Kiani, M. Shekarchi, A. Safari, Statistical and experimental analysis on the behavior of fiber reinforced concretes subjected to drop weight test, Constr. Build. Mater. 37 (2012) 360–369.
[86] A. Aghaeipour, M. Madhkhan, Effect of ground granulated blast furnace slag (GGBFS) on RCCP durability, Constr. Build. Mater. 141 (2017) 533–541.
[87] D. Mostofinejad, S.M. Hosseini, F. Nosouhian, T. Ozbakkaloglu, B.N. Tehrani, Durability of concrete containing recycled concrete coarse and fine aggregates and milled waste glass in magnesium sulfate environment, Journal of Building Engineering 29 (2020).